

Nonlinear Control of Mechanical Systems with an Unactuated Cyclic Variable

J.W. Grizzle⁺, C.H. Moog[§], and C. Chevallereau[§]

Abstract

Numerous robotic tasks associated with underactuation have been studied in the literature. For a large number of these in the plane, the mechanical models have a cyclic variable, the cyclic variable is unactuated, and all shape variables are independently actuated. This paper formulates and solves two control problems for this class of models. If the generalized momentum conjugate to the cyclic variable is not conserved, conditions are found for the existence of a set of outputs that yields an exponentially minimum-phase system with a one-dimensional zero dynamics, along with a dynamic extension that renders the system locally input-output decouplable. If the generalized momentum conjugate to the cyclic variable is conserved, a reduced system is constructed and conditions are found for the existence of a set of outputs that yields an empty zero dynamics, along with a dynamic extension that renders the system feedback linearizable. A common element in these two feedback problems is the construction of a scalar function of the configuration variables that has relative degree three with respect to one of the input components after an appropriate static feedback. The function arises by partially integrating the conjugate momentum. The results are illustrated on two balancing tasks and on a ballistic flip motion.

I. INTRODUCTION

Underactuated mechanical systems have fewer actuators than degrees of freedom. Underactuation is naturally associated with dexterity. For example, the act of standing with one foot flat on the ground is not viewed as particularly dexterous, whereas a headstand or *sur les pointes* (ballet) are considered dexterous. In the first case, since the foot is not in rotation with respect to the ground, the point of rotation is the ankle, which is actuated, as are each of the joints further up the tree; that is to say, normal standing involves a fully actuated system. On the other hand, in headstands or when on *pointe*, the contact point between the body and ground is acting as a pivot without actuation. These are underactuated systems. Similar arguments can be made for standing on a high wire, brachiation, a handstand on the rings, etc. In these examples, a typical control task would be to hold an equilibrium pose with (asymptotic) stability, or to execute a motion (e.g., a *relevé lent*, *battement*) without falling over (i.e., with internally bounded states).

Motions that include a ballistic phase are also often viewed as dexterous. Examples include dismounting from a highbar or platform diving. In these cases, the underactuation is manifest in the lack of contact with any surface. The ballistic phase is normally of short duration since reestablishing contact with a surface (e.g., ground, mat, water, ...) is an objective of the maneuver. A typical control problem would be to execute a predefined motion, with emphasis on achieving a final state that is compatible with an elegant landing on a mat (no rebounding or slipping), or re-entry into the water (no splash). Similar things can be said for back flips, tumbling, and somersaults.

⁺ **Corresponding author.** Control Systems Laboratory, Electrical Engineering and Computer Science Department, University of Michigan, Ann Arbor, MI 48109-2122, USA, grizzle@umich.edu

[§] IRCCyN, Ecole Centrale de Nantes, UMR CNRS 6597, BP 92101, 1 rue de la Noë, 44321 Nantes cedex 03, France, {Claude.Moog,Christine.Chevallereau}@irccyn.ec-nantes.fr

The objective of this paper is to contribute to the control of a special class of mechanical systems that are capable of executing such dexterous maneuvers in the plane. The literature on underactuated (a.k.a. super-articulated) systems and nonholonomic systems is vast. A few representative control works include the study of accessibility in [24], stabilization of equilibria through passivity techniques in [36] and energy shaping in [3], stabilization and tracking via backstepping in [46], the use of virtual constraints to achieve stabilization of orbits in [47], and path planning in [4]. Representative works in the robotics area are cited in Section II. One of the novelties of the present paper is to recognize that balancing on a pivot while executing a motion and planning a back flip share a common mathematical problem: designing a set of outputs that result in a *minimal* zero dynamics: exponentially minimum phase and one dimensional in the first case, and empty, in the second. In part, this is of course related to the *maximal* feedback linearization problem, which has been solved completely when static state feedback is considered [28], while only partial results are known when dynamic state feedback is allowed, *c.f.* [13], [26] and references therein. The additional requirement being achieved here is that the “non-feedback linearizable part” of the system is exponentially stable, and no general results are available on this aspect.

Section II identifies a special class of simple mechanical systems with one degree of underactuation that underlies the study of dexterous maneuvers in the plane as discussed previously. The key feature is that the systems possess a cyclic variable and this variable is unactuated [34]. Section III formulates and solves two related control problems. If the generalized momentum conjugate to the cyclic variable is not conserved, conditions are found for the existence of a set of outputs that yield an exponentially minimum phase system with a one-dimensional zero dynamics, along with a dynamic extension that renders the system locally input-output decouplable. When these two properties are met, it is well known that asymptotic tracking of an open set of output trajectories is possible, with all internal states remaining bounded [22]. If the generalized momentum conjugate to the cyclic variable is conserved, a reduced system is constructed and conditions are found for the existence of a set of outputs that yields an empty zero dynamics, along with a dynamic extension that renders the system input-output decouplable. When these two properties are met, it is well known that local dynamic state feedback linearization is possible [22]. *In both of these feedback problems, the principal contribution is the construction of a scalar function of the configuration variables that has relative degree three with respect to one of the input components after an appropriate static state feedback* [5]. The theoretical results are illustrated on three simple examples in Section IV. The purpose of the first example is to emphasize the role of the potential energy in determining whether generalized momentum is conserved, and to demonstrate the computations needed to apply the results of the paper in the simplest possible setting. The Acrobot is turned on its side. This removes gravity and induces conservation of angular momentum about the pivot point, which is an obstacle to stabilization of any equilibrium by a smooth

feedback. Stabilizability is restored through the attachment of a spring between the first link and the reference frame. The second example provides a non-trivial illustration of the principal results for a system with multiple inputs. Asymptotic stabilization about an equilibrium is achieved for a serial, three-link, planar mechanism attached to a pivot in a vertical plane. Asymptotic tracking is also illustrated through deep knee bends while balancing on the pivot (equivalently, press handstands on a highbar). The last example illustrates how locally linearizing coordinates can simplify the path planning problem for a ballistic flip motion [17]. The paper is wrapped up with some additional discussion of the results in Section V and concluding remarks in Section VI.

II. MOTIVATING CLASSES OF SYSTEMS

This section uses two classes of systems to set the stage for the mathematical and control developments that follow. The first class consists of $N \geq 2$ planar rigid bodies connected in a tree structure—no closed kinematic chains—with the base attached to an inertial reference frame via a pivot, that is, an unactuated revolute joint. It is supposed that each link has nonzero mass, and that each connection of two links is independently actuated so that the system has one degree of underactuation (N degrees of freedom with $N - 1$ independent actuators). It is further supposed that all joints are frictionless, but this assumption is really only important at the pivot. Figure 1 shows an example of such a system. Though not indicated in the figure, massless springs may be attached between links and between links and the inertial reference frame; prismatic joints between links are also allowed. This class of systems clearly includes the Acrobot [48], [2], [33], the brachiating robots of [42], [16], [31], [32], the gymnast robots of [29], [35], [53] when pivoting on a highbar, and the stance phase models of Raibert’s one-legged hopper [38], [23], [1], [6], [15], [30] as well as RABBIT [11], [9], [10], [37], [8]. The control objectives will be to stabilize the system about an equilibrium point or to track a set of reference trajectories with internal stability. The second class of systems consists of $N \geq 2$ planar rigid bodies, once again connected in a tree structure, but this time, it is assumed that the mechanism is undergoing ballistic motion. As before, it is supposed that each link has nonzero mass and each connection of two links is independently actuated. In addition, it is assumed that there are no springs between any link and an inertial reference frame. Such a system has three degrees of underactuation: $N + 2$ degrees of freedom and $N - 1$ independent actuators. Figure 2 shows an example of such a system. This class of systems clearly includes the gymnast robot of [29] when dismounting from the highbar, the planar diver of [18], the flip gait of the robot in [17], the ballistic phase of the 4-link planar robot in [43], and the ballistic phase of running in planar biped robots [9] and Raibert’s hopper [38], [23], [1], [6], [15]. The control objective will be to maximally linearize the system so as to facilitate the construction of a trajectory that transfers the state of the system from one point to another in finite time.

Consider the N -link system shown in Figure 1, along with the indicated coordinates, $q = (q_0, q_1, \dots,$

q_{N-1}), where, for convenience, the reference frame has been attached at the pivot point. The kinetic energy is quadratic, $K = \frac{1}{2}\dot{q}^T D(q)\dot{q}$, with D positive definite. Since the kinetic energy is independent of the orientation of the reference frame, D is independent of q_0 ; that is $\frac{\partial D(q)}{\partial q_0} \equiv 0$. The coordinate q_0 is said to be cyclic [19]. The form of the potential energy V depends on whether the system is evolving under the action of gravity (for example, in a vertical plane versus a horizontal plane) and whether or not springs have been attached at the joints. Electromagnetic and electrostatic forces are excluded, and hence, the potential energy depends only on the configuration variables. Denote the Lagrangian by $L = K - V$, and assume that the system is actuated such that

$$\frac{d}{dt} \frac{\partial L}{\partial \dot{q}_k} - \frac{\partial L}{\partial q_k} = \begin{cases} 0 & k = 0 \\ u_k & k = 1, \dots, N-1 \end{cases}, \quad (1)$$

with $u_k \in \mathbb{R}$. The model thus takes the form

$$D(q)\ddot{q} + C(q, \dot{q})\dot{q} + G(q) = Bu, \quad (2)$$

where $B = \begin{bmatrix} 0 \\ I \end{bmatrix}$.

Consider next the N -link system shown in Figure 2, along with the indicated coordinates, $q_e = (q, x_c, y_c)$, where (x_c, y_c) are the Cartesian coordinates of the center of mass. Suppose further that there are no springs between a link and an inertial reference frame. Then the equations of motion decompose as

$$\begin{aligned} \bar{D}(q)\ddot{q} + \bar{C}(q, \dot{q})\dot{q} + \bar{G}(q) &= Bu \\ \ddot{x}_c &= 0 \\ \ddot{y}_c &= g_0, \end{aligned} \quad (3)$$

where in a vertical plane g_0 is the gravitational constant and if the system is evolving on a horizontal plane without friction, then $g_0 = 0$. As in the first class of systems considered, q_0 is also a cyclic variable of \bar{D} because the kinetic energy is independent of the chosen orientation of the inertial reference frame.

The important point is that the dynamics of the body coordinates, q , and the Cartesian coordinates of the center of mass, (x_c, y_c) , are decoupled. Since the center of mass coordinates are unactuated, the control of the system (3) can be reduced to the control of a system having one degree of underactuation as in (2) by eliminating the trivial dynamics $\ddot{x}_c = 0$, $\ddot{y}_c = g_0$. In this sense, the two systems in Figures 1 and 2 are very similar: they give rise to control problems for systems with $N \geq 2$ DOF, $(N-1)$ actuators, and the cyclic coordinate is unactuated. One way in which the systems are often different is that angular momentum about the center of mass of (3) is always conserved, whereas whether or not (2) has a conserved quantity depends heavily on the potential energy. For example, consider a system as in Figure 1 in a horizontal plane without friction; suppose furthermore there are no springs between any link and the inertial reference frame. Then the angular momentum about the pivot point is a conserved quantity, and thus this feature—conservation of angular momentum—is possible in (2) as well. Conservation of angular momentum gives rise to a nonholonomic constraint [24] and changes fundamentally the nature of the control problem.

In summary, the models of the systems represented by Figures 1 and 2 present the common feature of an unactuated, cyclic variable. The system (2) has one degree of underactuation whereas even though the system (3) has three degrees of underactuation, in the proper coordinates, the control problem decouples into the control of a system of the form (2) plus keeping track of the free evolution of the center of mass variables. These observations are used in the next section to motivate the class of models analyzed. As a final remark, it is worth noting that [34] has shown quite clearly that even for systems with two degrees of freedom, if the cyclic coordinate and the unactuated coordinate do not coincide—such as in the inverted pendulum on a cart—then the system possesses quite different properties from a control point of view.

III. CONTROL OF SIMPLE MECHANICAL SYSTEMS WITH AN UNACTUATED CYCLIC VARIABLE

Consider the classes of mechanical systems motivated in Section II. Roughly speaking, the goal is to determine a set of outputs that give rise to a zero dynamics of “smallest possible” dimension, and if this dimension is non-zero, also to assure that the zero dynamics is stable [5]. More precisely, in the case of a system where the generalized momentum conjugate to the cyclic variable is not conserved, a set of outputs will be found that leads to local dynamic input-output decouplability and a one-dimensional exponentially stable zero dynamics, and for systems where the conjugate momentum is conserved, a set of flat outputs [41], [14] will be determined; that is, a set of outputs will be found that leads to the construction of a regular dynamic feedback and a local change of coordinates in which the system is linear.

Before proceeding, it is worth noting that if outputs are chosen to correspond to the actuated variables, that is, $y_i = q_i$, for $i = 1, \dots, N - 1$, then each component has relative degree two and the associated decoupling matrix is clearly invertible (one says the system has vector relative degree $(2, \dots, 2)$ [22]). Such a choice leads to a two-dimensional zero dynamics, which, moreover, can be shown to be once again a Lagrangian system [52], and thus can never have an asymptotically stable equilibrium. One way to get around this problem is to construct a set of outputs such that the associated zero dynamics has dimension one, and hence is not Lagrangian. For special cases, [5] shows how to construct an output component that has relative degree three with respect to one of the input components after an appropriate static feedback. This idea is developed in much more generality here.

A. *Partial integration of a one-form*

This subsection presents a key result that will lead to the construction of outputs for the system (2) so that the associated zero dynamics has dimension one, and hence may admit an asymptotically stable equilibrium point. As will be seen in the next subsection, the abstract one-form considered here naturally arises from consideration of momentum. The result formalizes and extends previous work of [34] and [5].

Lemma 1: Consider a smooth N -dimensional manifold Q . Let $\tilde{\omega} \in T^*Q$ be a smooth one-form on Q and suppose there is a set of local coordinates $(q_0, q_1, \dots, q_{N-1})$ defined in an open neighborhood \mathcal{O} of a point $(q_0^*, q_1^*, \dots, q_{N-1}^*)$ in which $\tilde{\omega}$ has the form

$$\tilde{\omega} = dq_0 + \sum_{k=1}^{N-1} \alpha_k(q_1, \dots, q_{N-1})dq_k. \quad (4)$$

Then for any choice of $1 \leq m \leq N-1$, there exists a function $p_m : \mathcal{O} \rightarrow \mathbb{R}$ such that

$$\tilde{\omega} = dp_m \text{ mod } \text{span} \{dq_i | 1 \leq i \leq N-1, i \neq m\}. \quad (5)$$

Moreover, one such function is

$$p_m = q_0 - q_0^* + \int_{q_m^*}^{q_m} \alpha_m(q_1, \dots, q_{m-1}, \tau, q_{m+1}, \dots, q_{N-1})d\tau \quad (6)$$

Proof: The integral in (6) is well-defined at each point in \mathcal{O} because the integrand is smooth and the integral is evaluated over a closed and bounded interval. Since

$$dp_m = dq_0 + \alpha_m(q_1, \dots, q_{N-1})dq_m + \sum_{k=1, k \neq m}^{N-1} \int_{q_m^*}^{q_m} \frac{\partial \alpha_m(q_1, \dots, q_{m-1}, \tau, q_{m+1}, \dots, q_{N-1})}{\partial q_k} d\tau dq_k,$$

it follows immediately that, at each point in \mathcal{O} ,

$$\tilde{\omega} - dp_m \in \text{span} \{dq_i | 1 \leq i \leq N-1, i \neq m\}. \quad (7)$$

■

Remark 1: Given a collection of smooth real-valued functions $\{f_i | 1 \leq i \leq k\}$, $\text{span} \{df_i | 1 \leq i \leq k\}$ denotes the corresponding codistribution [22]; that is, the span is computed point-wise over \mathbb{R} . This applies to (5) and elsewhere in the paper. In (5), (7), and elsewhere, the modulo operation is interpreted to hold pointwise.

Remark 2: $(p_m, q_1, \dots, q_{N-1})$ is a valid set of coordinates on \mathcal{O} . Indeed,

$$q_0 = q_0^* + p_m - \int_{q_m^*}^{q_m} \alpha_m(q_1, \dots, q_{m-1}, \tau, q_{m+1}, \dots, q_{N-1})d\tau.$$

Said another way, the map that takes $(q_0, q_1, \dots, q_{N-1})$ to $(p_m, q_1, \dots, q_{N-1})$ is a diffeomorphism on \mathcal{O} .

Remark 3: If $p_m : \mathcal{O} \rightarrow \mathbb{R}$ satisfies (5) and $\gamma : \mathcal{O} \rightarrow \mathbb{R}$ satisfies $d\gamma \in \text{span} \{dq_i | 1 \leq i \leq N-1, i \neq m\}$, then obviously $\tilde{p}_m := p_m + \gamma$ also satisfies (5). This observation can be useful for simplifying the choice of p_m .

B. Model class and a normal form

Consider a (simple¹) N -DOF Lagrangian system with $(N-1) \geq 1$ independent actuators, where the unactuated variable is a cyclic coordinate of the kinetic energy. Specifically, let the configuration

¹Simple means that the kinetic energy is quadratic and the potential energy depends only on the configuration variables.

space be Q , an open connected subset of \mathbb{R}^N , with local coordinates denoted by $q = (q_0, q_1, \dots, q_{N-1})$, and take canonical coordinates (q, \dot{q}) on TQ . Let the kinetic energy be given by $K = \frac{1}{2}\dot{q}^T D(q)\dot{q}$, where D is positive definite and smooth everywhere on Q , and satisfies $\frac{\partial D(q)}{\partial q_0} \equiv 0$ (i.e., q_0 is cyclic). Let the potential energy, V , depend only on the configuration variables and be smooth. Denote the Lagrangian by $L = K - V$ and assume that the system is actuated according to (1). The model can then be written as in (2). Subsequent analysis and feedback design are more easily accomplished if the system is first transformed into the Spong normal form [49], [40]

$$\begin{aligned}\ddot{q}_0 &= \sum_{k=1}^{N-1} J_k(q_1, \dots, q_{N-1})v_k + R(q, \dot{q}) \\ \ddot{q}_1 &= v_1 \\ &\vdots \\ \ddot{q}_{N-1} &= v_{N-1},\end{aligned}\tag{8}$$

where $J_k = -\frac{d_{0,k}}{d_{0,0}}$, $d_{0,k}$, $k = 0, \dots, N-1$ are the entries in the first row of D . See the Appendix for the required (regular) static state feedback transformation. Note that everywhere D is positive definite, $d_{0,0}$ is never zero. Note also that J_k does not depend on q_0 because q_0 is cyclic.

Denote the generalized momentum conjugate to q_0 [19] by $\sigma = \frac{\partial L}{\partial \dot{q}_0}$. Because the kinetic energy is quadratic and the potential energy depends only on the configuration variables, it follows that

$$\sigma = \sum_{k=0}^{N-1} d_{0,k}(q_1, \dots, q_{N-1})\dot{q}_k.\tag{9}$$

From the assumption on the actuation and the assumption that q_0 is cyclic,

$$\dot{\sigma} = -\frac{\partial V}{\partial q_0}(q).\tag{10}$$

For later use, note that (10) implies that the relative degree of σ is at least three². Using (9) and (10) to express the Spong normal form in terms of the state variables $q_0, q_1, \dots, q_N, \sigma, \dot{q}_1 \dots \dot{q}_N$, instead of $q_0, \dots, q_N, \dot{q}_0 \dots \dot{q}_N$, shows that (2) is (globally) static state feedback equivalent to

$$\begin{aligned}\dot{q}_0 &= \frac{\sigma}{d_{0,0}(q_1, \dots, q_{N-1})} + \sum_{k=1}^{N-1} J_k(q_1, \dots, q_{N-1})\dot{q}_k \\ \dot{\sigma} &= -\frac{\partial V}{\partial q_0}(q) \\ \ddot{q}_j &= v_j \quad j = 1, \dots, N-1,\end{aligned}\tag{11}$$

which will be called the *modified* Spong normal form. Since only a change of state variables has been made, the feedback required to go from (2) to (11) is the same as that used in (8).

Associate to σ the one-form $\omega = \sum_{k=0}^{N-1} d_{0,k}(q_1, \dots, q_{N-1})dq_k$, and the normalized one-form $\omega_{norm} = dq_0 + \sum_{k=1}^{N-1} \frac{d_{0,k}}{d_{0,0}}(q_1, \dots, q_{N-1})dq_k$. Applying Lemma 1 for $m = 1$, define the function

$$p_1 = q_0 - q_0^* + \int_{q_1^*}^{q_1} \frac{d_{0,1}}{d_{0,0}}(\tau, q_2, \dots, q_{N-1})d\tau.\tag{12}$$

²If friction were allowed at the unactuated joint, then the relative degree would in general be only one.

Direct computation then leads to

$$\frac{dp_1}{dt} = \frac{\sigma}{d_{0,0}(q_1, \dots, q_{N-1})} + \sum_{k=2}^{N-1} \beta_k(q_1, \dots, q_{N-1}) \dot{q}_k, \quad (13)$$

where,

$$\beta_k(q_1, \dots, q_{N-1}) = \int_{q_1^*}^{q_1} \frac{\partial}{\partial q_k} \frac{d_{0,1}}{d_{0,0}}(\tau, q_2, \dots, q_{N-1}) d\tau - \frac{d_{0,k}}{d_{0,0}}(q_1, \dots, q_{N-1}).$$

Note that since \dot{p}_1 does not depend on \dot{q}_1 , it must be differentiated at least twice more before v_1 appears; in other words, p_1 has at least relative degree three with respect to v_1 .

This concludes the preliminary analysis required for subsequent feedback design.

C. Systems where the generalized momentum conjugate to the cyclic variable is not conserved

It is first assumed that σ , the generalized momentum conjugate to q_0 , is not constant along solutions of the model (1); that is

$$G_0(q) := -\frac{\partial V}{\partial q_0}(q) \neq 0. \quad (14)$$

It is also assumed that there exists a static equilibrium point $(q^e, 0)$ corresponding to some constant value of the control, and that when defining p_1 via (12), q^* is taken as q^e so that p_1 vanishes³ at the equilibrium point. In this case, conditions will be identified under which the set of outputs,

$$\begin{aligned} y_1 &= Kp_1 + \sigma \\ y_2 &= q_2 - q_2^e \\ &\vdots \\ y_{N-1} &= q_{N-1} - q_{N-1}^e, \end{aligned} \quad (15)$$

$K \in \mathbb{R}$ a constant, yields an exponentially minimum phase system. More precisely, conditions will be given such that the zero dynamics is well defined in a neighborhood of the given equilibrium point, has dimension one, and is exponentially stable for all $K > 0$, and moreover, the system is dynamically input-output decouplable (equivalently, invertible).

Before proceeding with the analysis, the intuition behind this choice of outputs is discussed. As stated earlier, a more standard choice of outputs would be $y_i = q_i - q_i^e$, for $i = 1, \dots, N-1$, where each component has relative degree two. Such a choice leads to a two-dimensional zero dynamics, which can be shown to be once again a Lagrangian system [52], and thus can never have an asymptotically stable equilibrium. By seeking an output component with a relative degree higher than two, the dimension of the zero dynamics can be reduced, opening up the possibility of either having no zero dynamics at all, or, of creating one that is scalar and asymptotically stable. For the class of systems being studied, no output function of relative degree four has been found (see Section V-B for more discussion on this point). The most obvious relative degree three function available is the conjugate

³Alternatively, let q^* be arbitrary, for example, zero, and define $y_1 = K(p_1 - p_1^e) + \sigma$, where p_1^e is the value at the equilibrium point, q^e .

momentum, σ , which is a linear combination of the velocity components. If the first component of the outputs were modified to $y_1 = \sigma$, the resulting zero dynamics manifold would include a one-dimensional submanifold of equilibria associated with $G_0(q_0, q_1, q_2^e, \dots, q_{N-1}^e) = 0$, and thus asymptotic stability of the zero dynamics would be impossible. Inspired by [5], by associating σ to a one-form and then partially integrating it, a function p_1 was determined that depends only on the configuration variables and has at least relative degree three with respect to one of the input components (after a static feedback was used to put the system in Spong normal form). Hence *any* function of p_1 and σ has at least relative degree three with respect to that input component. Moreover, by (13), if $\dot{q}_i = 0$, for $i = 2, \dots, N-1$, then σ is proportional to \dot{p}_1 through the strictly positive quantity $d_{0,0}$. Thus the choice $y_1 = Kp_1 + \sigma$, $K > 0$, and $y_i = q_i - q_i^e$, for $i = 2, \dots, N-1$, should lead to the asymptotically stable zero dynamics $\dot{p}_1 = -Kp_1/d_{0,0}$.

To continue with the control law design, apply a dynamic extension to (11) via

$$\begin{aligned} v_1 &= w_1 \\ \dot{v}_2 &= w_2 \\ &\vdots \\ \dot{v}_{N-1} &= w_{N-1}. \end{aligned} \tag{16}$$

Note that an integrator has not been added on v_1 , and this is because p_1 is designed to have relative degree three with respect to v_1 , while it only has relative degree two with respect to v_2, \dots, v_{N-1} . With the dynamic extension, p_1 will have relative degree three with respect to w .

Clearly, $y_k^{(3)} = w_k$, for $2 \leq k \leq N-1$. It remains to differentiate the first output component. Using (13), yields

$$\frac{dy_1}{dt} = K \left[\frac{\sigma}{d_{0,0}(q_1, \dots, q_{N-1})} + \sum_{k=2}^{N-1} \beta_k(q_1, \dots, q_{N-1}) \dot{q}_k \right] - \frac{\partial V(q)}{\partial q_0}. \tag{17}$$

The arguments (q_1, \dots, q_{N-1}) will now be dropped so that the formulas remain compact and readable. Differentiating (17) again yields

$$\frac{d^2 y_1}{dt^2} = K \left[\frac{\dot{\sigma}}{d_{0,0}} - \frac{\sigma}{d_{0,0}^2} \dot{d}_{0,0} + \sum_{k=2}^{N-1} (\dot{\beta}_k \dot{q}_k + \beta_k \ddot{q}_k) \right] - \frac{\partial^2 V(q)}{\partial q \partial q_0} \dot{q}. \tag{18}$$

Due to the dynamic extension (16), (q_2, \dots, q_{N-1}) have relative degree three while q_1 only has relative degree two, thus the inputs do not appear in $\frac{d^2 y_1}{dt^2}$. Differentiating once more and keeping track only of the terms where the inputs appear yield

$$\frac{d^3 y_1}{dt^3} = (*) + M_{1,1} w_1 + \sum_{k=2}^{N-1} K \beta_k w_k \tag{19}$$

$$M_{1,1} = -K \frac{\sigma}{d_{0,0}^2} \frac{\partial d_{0,0}}{\partial q_1} + K \sum_{k=2}^{N-1} \left(\frac{\partial \beta_k}{\partial q_1} \dot{q}_k \right) - \frac{\partial^2 V}{\partial q_0^2} J_1 - \frac{\partial^2 V}{\partial q_1 \partial q_0} \tag{20}$$

and therefore the decoupling matrix is

$$M := \begin{bmatrix} M_{1,1} & K [\beta_2, \dots, \beta_{N-1}] \\ 0 & I_{(N-2) \times (N-2)} \end{bmatrix}. \tag{21}$$

The decoupling matrix is thus invertible at a given point if, and only if, $M_{1,1}$ is non-zero at that point. In a neighborhood of an equilibrium point $(q^e, 0)$, $M_{1,1}$ is non-zero if, and only if,

$$\left(\frac{\partial^2 V}{\partial q_0^2} \frac{d_{0,1}}{d_{0,0}} - \frac{\partial^2 V}{\partial q_1 \partial q_0} \right) \Big|_{q^e} \neq 0. \quad (22)$$

Wherever the decoupling matrix is invertible, the zero dynamics is locally well defined and the set of differentials, $\{dy_k^{(j)}, j = 0, 1, 2; 1 \leq k \leq N - 1\}$, is independent [22], and hence has dimension $3N - 3$. The system (11) with the dynamic extension (16) has dimension $3N - 2$, and thus the zero dynamics has dimension one.

To determine the zero dynamics, it is enough to find a function whose differential is independent of $\{dy_k^{(j)}, j = 0, 1, 2, 1 \leq k \leq N - 1\}$. In the Appendix, it is shown that p_1 is an appropriate choice. On the zero dynamics manifold (that is, when $y \equiv 0$), $\sigma = -Kp_1$, $q_1 = q_1(p_1, q^e)$, and $q_k - q_k^e = \dot{q}_k = 0$, $2 \leq k \leq N - 1$. Thus, from (13) (see also (78) in the Appendix), in a neighborhood of an equilibrium point where $M_{1,1} \neq 0$, the zero dynamics is

$$\dot{p}_1 = -\frac{K}{d_{0,0}(q_1(p_1, q^e), q_2^e, \dots, q_{N-1}^e)} p_1. \quad (23)$$

Since $d_{0,0}$ is positive, the zero dynamics is exponentially stable for all $K > 0$.

The main result is now summarized in the following theorem.

Theorem 1: Consider the simple mechanical system (2) with $N \geq 2$ DOF, $N - 1$ independent actuators, and the unactuated coordinate is cyclic. Associate to the system the outputs defined in (15), for $K > 0$. Then at any equilibrium point at which $M_{1,1}$ in (20) is non-zero, the system is

- i) exponentially minimum phase and
- ii) dynamically input-output decouplable.

Moreover, once the system is transformed into Spong normal form as in (8), or into the modified Spong normal form as in (11), then the dynamic extension (16) renders it statically input-output decouplable.

Remark 4: From [22], exponential minimum phase plus static input-output decouplability after a dynamic extension implies the existence of a feedback that induces asymptotic tracking of output trajectories with internally bounded states. See the three-link robot in Section IV-C.2 for an example.

Remark 5: If p_m in (12) is selected with $m \neq 1$, then the dynamic extension becomes

$$\begin{aligned} v_m &= w_m \\ \dot{w}_k &= w_k, \quad 1 \leq k \leq N - 1, \quad k \neq m, \end{aligned} \quad (24)$$

$$\frac{d^3 y_1}{dt^3} = (*) + \left\{ -K \frac{\sigma}{d_{0,0}^2} \frac{\partial d_{0,0}}{\partial q_m} + K \sum_{k=1, k \neq m}^{N-1} \frac{\partial \beta_k}{\partial q_m} \dot{q}_k - \frac{\partial^2 V}{\partial q_0^2} J_m - \frac{\partial^2 V}{\partial q_m \partial q_0} \right\} w_m + \sum_{k=1, k \neq m}^{N-1} K \beta_k w_k,$$

and the decoupling matrix is invertible in a neighborhood of an equilibrium point $(q^e, 0)$ if, and only if,

$$\left(\frac{\partial^2 V}{\partial q_0^2} \frac{d_{0,m}}{d_{0,0}} - \frac{\partial^2 V}{\partial q_m \partial q_0} \right) \Big|_{q^e} \neq 0. \quad (25)$$

Choosing different values of m may be useful for avoiding singularities.

D. Systems where the generalized momentum conjugate to the cyclic variable is conserved

It is now assumed that σ , the generalized momentum conjugate to q_0 , is constant along solutions of the model; that is

$$G_0(q) := -\frac{\partial V}{\partial q_0}(q) \equiv 0, \quad (26)$$

which is equivalent to $\dot{\sigma} \equiv 0$. In (11), σ can be treated as a constant, yielding the reduced order model

$$\begin{aligned} \dot{q}_0 &= \frac{\sigma}{d_{0,0}(q_1, \dots, q_{N-1})} + \sum_{k=1}^{N-1} J_k(q_1, \dots, q_{N-1}) \dot{q}_k \\ \ddot{q}_j &= v_j \quad j = 1 \dots N-1. \end{aligned} \quad (27)$$

Let $q^* \in Q$ be given and define p_1 as in (12). In this case, conditions will be found such that the system (27) with outputs

$$\begin{aligned} y_1 &= p_1 \\ y_2 &= q_2 - q_2^* \\ &\vdots \\ y_{N-1} &= q_{N-1} - q_{N-1}^*, \end{aligned} \quad (28)$$

is locally, dynamically, feedback linearizable. Note that (28) is a simplification of (15) arising from $\dot{\sigma} \equiv 0$.

As in Section III-C, apply the dynamic extension (16) to (27). Once again, $y_k^{(3)} = w_k$, for $2 \leq k \leq N-1$ and it remains to differentiate the first output component. From (17)-(19), by taking $K = 1$ and $\frac{\partial V}{\partial q_0}(q) \equiv 0$, it follows that

$$\frac{dy_1}{dt} = \frac{\sigma}{d_{0,0}} + \sum_{k=2}^{N-1} \beta_k \dot{q}_k \quad (29)$$

$$\frac{d^2 y_1}{dt^2} = -\frac{\sigma}{d_{0,0}^2} \dot{d}_{0,0} + \sum_{k=2}^{N-1} (\dot{\beta}_k \dot{q}_k + \beta_k \ddot{q}_k) \quad (30)$$

$$\frac{d^3 y_1}{dt^3} = (*) + M_{1,1} w_1 + \sum_{k=2}^{N-1} \beta_k w_k, \quad (31)$$

where

$$M_{1,1} = -\frac{\sigma}{d_{0,0}^2} \frac{\partial d_{0,0}}{\partial q_1} + \sum_{k=2}^{N-1} \left(\frac{\partial \beta_k}{\partial q_1} \dot{q}_k \right). \quad (32)$$

Thus, the decoupling matrix is

$$M := \begin{bmatrix} M_{1,1} & [\beta_2, \dots, \beta_{N-1}] \\ 0 & I_{(N-2) \times (N-2)} \end{bmatrix} \quad (33)$$

and is invertible in a neighborhood of a given point if, and only if, $M_{1,1}$ is non-zero at that point. In a neighborhood of a point where the decoupling matrix is invertible, the sum of the relative degrees of the outputs is $3(N-1)$, which equals the sum of the dimensions of (27) and (16). It follows that (27) with outputs (28) has no zero dynamics [22], and thus any regular static feedback that input-output linearizes (27), (28) and (16), also renders the closed-loop system input-to-state linear in the coordinates $(y_k^{(j)} | 1 \leq k \leq N-1, 0 \leq j \leq 2)$; the associated Brunovsky canonical form is $y_k^{(3)} = \bar{w}_k$, $1 \leq k \leq N-1$.

Theorem 2: Consider a simple mechanical system (2) with $N \geq 2$ DOF, $N - 1$ independent actuators, and the unactuated coordinate is cyclic. Suppose that the generalized momentum conjugate to the cyclic coordinate is conserved along the motions of the system, so that the reduced system (27) can be defined. Associate to (27) the outputs defined in (28). Then in a neighborhood of any point at which $M_{1,1}$ in (32) is non-zero, the following hold:

- i) the system (27) is dynamically feedback equivalent to a controllable linear system;
- ii) the system (27) is the strongly accessible part of (2), and $\dot{\sigma} = 0$ can be viewed as a representation of the uncontrollable part;
- iii) the system (2) is dynamically feedback equivalent to a linear system with a one-dimensional uncontrollable part; and
- iv) the system (27) with outputs (28) is dynamically input-output decouplable and has no zero dynamics.

Moreover, the dynamic extension (16) renders (27) statically feedback linearizable.

Corollary 1: The same results hold for (3) with the exception that the uncontrollable part has dimension five:

$$\begin{aligned} \dot{\sigma} &= 0 \\ \ddot{x}_c &= 0 \\ \ddot{y}_c &= g_0, \end{aligned} \tag{34}$$

where g_0 is a constant.

IV. EXAMPLES

This section will illustrate the theoretical results of Section III on systems of the type depicted in Figures 1 and 2. The systems are chosen to be simple enough that the calculations are straightforward and sufficiently complex to illustrate a range of possible applications of the main theorems. The first example treats a robot with two rigid links connected via an actuated revolute joint and attached at one end to a pivot; that is, the acrobot. A novel feature is that the robot is placed on a frictionless horizontal plane to remove gravity. If nothing else were done, the angular momentum about the attachment point would be conserved, so stabilization about an equilibrium would not be possible. A spring is therefore added between the world frame and the first link, and a stabilizing controller is then designed through the use of Theorem 1. The second example treats a robot consisting of three serial links connected by independently actuated revolute joints, attached to a pivot, and constrained to evolve in a vertical plane. For this system, the results of [5], [34] are not applicable for designing a stabilizing controller. Theorem 1 is applied to design a controller that achieves stabilization about an equilibrium point and asymptotic tracking of trajectories. The last problem studied focuses on

ballistic motion in a vertical plane, which is a key part of a model of running. The model assumes a robot with two rigid links connected via an actuated revolute joint. The angular momentum about the center of mass is conserved, creating a nonholonomic constraint. Corollary 1 is applied to feedback linearize the accessible part of the system. The linear representation of the dynamics is shown to be advantageous for path planning. The singularities that prevent the system from being globally linearized are explicitly noted and how to plan a path through such a singularity is illustrated.

A. Computing the outputs

The key to applying the results of Section III is the explicit computation of the function p_1 in (12) used to define the outputs. For all of the examples treated here, plus a wide range of other examples, the computation of this function is handled by the following lemma. The proof by direct symbolic integration is not given.

Lemma 2: Consider a simple mechanical system of the form (2), with $N \geq 2$ DOF and mass inertia matrix D . Suppose that $d_{0,0}$ and $d_{0,1}$ can be expressed as

$$\begin{aligned} d_{0,0} &= a_{00} + a_{01} \cos(q_1) + a_{02} \sin(q_1) \\ d_{0,1} &= a_{10} + a_{11} \cos(q_1) + a_{12} \sin(q_1), \end{aligned} \quad (35)$$

where $a_{ij} = a_{ij}(q_2, \dots, q_{N-1})$. Then for $q^* = 0$ and $-\pi < q_1 < \pi$, (12) can be evaluated explicitly as

$$p_1 = q_0 + \frac{c_1}{c_2} q_1 + \varphi_1 \circ \tan\left(\frac{q_1}{2}\right) + \varphi_2 \circ \tan\left(\frac{q_1}{2}\right), \quad (36)$$

where,

$$\begin{aligned} \varphi_1(x) &= 2\left(\frac{a_{10}}{c_3} - \frac{a_{00}c_1}{c_2c_3}\right) \arctan\left(\frac{(a_{00}-a_{01})x+a_{02}}{c_3}\right) \\ \varphi_2(x) &= \frac{(a_{02}a_{11}-a_{01}a_{12})}{c_2} \ln(a_{00}(1+x^2) + a_{01}(1-x^2) + 2a_{02}x) - \frac{a_{02}a_{11}}{c_2} \ln(1+x^2) \\ c_1 &= a_{01}a_{11} + a_{12}a_{02} \\ c_2 &= a_{01}^2 + a_{02}^2 \\ c_3 &= \sqrt{a_{00}^2 - a_{01}^2 - a_{02}^2}. \end{aligned} \quad (37)$$

Remark 6: If $N = 2$ and either $a_{02} = a_{12} = 0$ or $a_{01} = a_{11} = 0$, then $\varphi_2 \equiv 0$. In this case, the results simplify to [34].

Remark 7: For a general point of interest $q^* \neq 0$, (12) can be evaluated as

$$p_1 = (q_0 - q_0^*) + \frac{c_1}{c_2}(q_1 - q_1^*) + \varphi_1 \circ \tan\left(\frac{q_1}{2}\right) + \varphi_2 \circ \tan\left(\frac{q_1}{2}\right) - \varphi_1 \circ \tan\left(\frac{q_1^*}{2}\right) - \varphi_2 \circ \tan\left(\frac{q_1^*}{2}\right),$$

which is just p_1 in (36) minus the same function evaluated at q^* .

B. Planar Two-link Structure Attached to a Pivot

The purpose of the example is to emphasize the role of the potential energy in determining whether generalized momentum is conserved, and to demonstrate in the simplest possible setting the computations needed to apply Theorem 1 in order to achieve asymptotic stabilization of an equilibrium. The

robot consists of two point masses connected by two rigid, massless links, with the links joined by an actuated revolute joint (the use of a distributed mass model would not change any of the following analysis). The connection to the pivot is unactuated and frictionless.

The configuration variables are chosen as q_0 and q_1 , where q_0 is the angle of the first link referenced to a world frame attached to the pivot point and q_1 is the relative angle between links one and two. A linear spring of stiffness K_s is introduced between the first link and the world frame, with rest position $q_0 = 0$. The plane of movement is assumed to be horizontal, and thus the acceleration due to gravity is $g_0 = 0$.

B.1 Mathematical representation

The dynamic model is easily obtained with the method of Lagrange and verifies that q_0 is a cyclic variable. The complete dynamic model is not given; instead, the system is immediately written in modified Spong normal form (11) as

$$\begin{aligned}\dot{q}_0 &= \frac{\sigma}{d_{0,0}} - \frac{d_{0,1}}{d_{0,0}} \dot{q}_1 \\ \dot{\sigma} &= G_0 \\ \ddot{q}_1 &= v_1\end{aligned}\tag{38}$$

where,

$$\begin{aligned}d_{0,0} &= a_{00} + a_{01} \cos(q_1) \\ d_{0,1} &= a_{10} + a_{11} \cos(q_1) \\ a_{00} &= (m_1 + m_2)L_1^2 + m_2L_2^2 \\ a_{01} &= 2a_{11} \\ a_{10} &= m_2L_2^2 \\ a_{11} &= m_2L_1L_2 \\ G_0 &= -\frac{\partial V}{\partial q_0} = -K_s q_0.\end{aligned}\tag{39}$$

In the above, note that σ , given by (9), is the usual angular momentum of the robot about the attachment point. Since the robot is constrained to a horizontal plane, if the spring constant were zero, then angular momentum would be conserved and asymptotic stabilization to an equilibrium point would be impossible with a smooth static state feedback.

B.2 Control Law Design

The control law design consists of the preliminary feedback needed to place the system in (modified) Spong normal form (as explained in the Appendix), the definition of an output, and a second static state feedback used to linearize and stabilize the resulting input-output map. For the two-link robot, the output was selected as

$$y = K(p_1 - p_1^e) + \sigma,\tag{40}$$

where $K > 0$ is to be chosen,

$$p_1 = q_0 + \frac{a_{11}}{a_{01}} q_1 + 2 \left(\frac{a_{10}}{\sqrt{a_{00}^2 - a_{01}^2}} - \frac{a_{00}a_{11}}{a_{01}\sqrt{a_{00}^2 - a_{01}^2}} \right) \arctan \left(\frac{a_{00} - a_{01}}{\sqrt{a_{00}^2 - a_{01}^2}} \tan\left(\frac{q_1}{2}\right) \right),\tag{41}$$

and p_1^e is the value of p_1 at the equilibrium of interest, q^e .

For single input systems, the dynamic extension (16) is trivial: $v_1 = w_1$. Since it only amounts to relabelling the input, it is dropped. Direct calculation confirms that y has relative degree three:

$$\begin{aligned} \dot{y} &= K \frac{\sigma}{d_{0,0}} + K_s q_0 \\ \ddot{y} &= K \left[\frac{K_s q_0}{d_{0,0}} - \frac{\sigma}{d_{0,0}^2} \frac{\partial d_{0,0}}{\partial q_1} \dot{q}_1 \right] + K_s \left[\frac{\sigma - d_{0,1} \dot{q}_1}{d_{0,0}} \right] \\ y^{(3)} &= Mv + N, \end{aligned} \quad (42)$$

where,

$$\begin{aligned} M &= -K \frac{\sigma}{d_{0,0}^2} \frac{\partial d_{0,0}}{\partial q_1} - K_s \frac{d_{0,1}}{d_{0,0}} \\ N &= K \left[K_s \frac{\dot{q}_0}{d_{0,0}} - 2 \frac{K_s q_0}{d_{0,0}^2} \frac{\partial d_{0,0}}{\partial q_1} \dot{q}_1 + \frac{\sigma}{d_{0,0}^3} \left(\frac{\partial d_{0,0}}{\partial q_1} \dot{q}_1 \right)^2 - \frac{\sigma}{d_{0,0}^2} \frac{\partial^2 d_{0,0}}{\partial^2 q_1} \dot{q}_1^2 \right] + \\ &K_s \left[\frac{K_s q_0}{d_{0,0}} - \frac{\partial d_{0,1}}{\partial q_1} \frac{q_1^2}{d_{0,0}} - \left(\frac{\sigma - d_{0,1} \dot{q}_1}{d_{0,0}^2} \right) \frac{\partial d_{0,0}}{\partial q_1} \dot{q}_1 \right]. \end{aligned} \quad (43)$$

Suppose that $M(q^e) \neq 0$. Let real scalars \bar{K}_2 , \bar{K}_1 and \bar{K}_0 be chosen such that $y^{(3)} + \sum_{j=0}^2 \bar{K}_j y^{(j)} = 0$ is exponentially stable. Then (43) leads to the locally input-output linearizing and exponentially stabilizing control law [22]

$$v = \frac{1}{M(q)} \left[-N(q, \dot{q}) - \bar{K}_2 \ddot{y} - \bar{K}_1 \dot{y} - \bar{K}_0 y \right]. \quad (44)$$

The actual torque applied to the actuated joint is computed from (75) of the Appendix.

B.3 Simulation

For the simulations, the robot is assumed constrained to a horizontal plane ($g_0 = 0$), the spring attaching the first link to the reference frame is assumed linear with stiffness $K_s = 5$, and the model parameters are selected as $L_1 = 0.5$, $L_2 = 0.75$, $m_1 = 7$, and $m_2 = 7$. The equilibrium point was chosen as $q_0^e = 0$, $q_1^e = -\pi/4$, which corresponds to $p_1^e = -0.4068$, and satisfies $M(q^e) \neq 0$. The scalars \bar{K}_j were arbitrarily chosen to place the eigenvalues of the error equation at -1.3 . The free parameter in the output was arbitrarily set to $K = 4$. Since $d_{0,0}(q^e) \approx 5$, the zero dynamics has a slightly slower speed of convergence than the output error equation.

The state feedback controller (44) was simulated for the initial condition $q_0 = \pi/4$, $q_1 = \pi/4$, $\dot{q}_0 = 0$, $\dot{q}_1 = 0$. Figure 4 shows the evolution of the commanded output and its derivatives along with the evolution of the configuration variables of the robot. The output rapidly converges to zero and the configuration variables converge to the desired equilibrium point. An animation of the motion is available at [20].

C. Planar Three-Link Serial Structure Attached to a Pivot

This example treats the planar three-link robot depicted in Figure 5. The robot consists of three point masses connected by three rigid, massless links, with the links joined by an actuated revolute joint. The connection to the pivot is unactuated and frictionless. The links are labelled L_1 through L_3

starting from the pivot and the masses are similarly labelled m_1 through m_3 . The parameter values given in Table I were selected to approximate the biped robot RABBIT with the legs held together [8]. The configuration variables are chosen as q_0 through q_2 , where q_0 is the angle of the first link referenced to a world frame attached to the pivot point, q_1 is the relative angle between links one and two, and q_2 is the relative angle between links two and three. No springs are used. The plane of movement is assumed to be vertical, and thus the acceleration due to gravity is $g_0 = 9.81$.

The example further illustrates the application of Theorem 1 through the use of an output component that has relative degree three with respect to only one of the input components and the use of a non-trivial dynamic extension in the design of the feedback controller. Both local asymptotic tracking and exponential stabilization to an equilibrium point are demonstrated.

C.1 Mathematical representation

The complete dynamic model is easily obtained using the method of Lagrange and yields immediately the modified Spong normal form (11) as

$$\begin{aligned}\dot{q}_0 &= \frac{\sigma}{d_{0,0}} - \frac{d_{0,1}}{d_{0,0}}\dot{q}_1 - \frac{d_{0,2}}{d_{0,0}}\dot{q}_2 \\ \dot{\sigma} &= G_0 \\ \ddot{q}_1 &= v_1 \\ \ddot{q}_2 &= v_2,\end{aligned}\tag{45}$$

where,

$$\begin{aligned}a_{00} &= (m_1 + m_2 + m_3)L_1^2 + (m_2 + m_3)L_2^2 + m_3L_3^2 + 2m_3L_2L_3\cos(q_2) \\ a_{01} &= 2(m_2 + m_3)L_1L_2 + 2m_3L_1L_3\cos(q_2) \\ a_{02} &= -2m_3L_1L_3\sin(q_2) \\ a_{10} &= (m_2 + m_3)L_2^2 + m_3L_3^2 + 2m_3L_2L_3\cos(q_2) \\ a_{11} &= (m_2 + m_3)L_1L_2 + m_3L_1L_3\cos(q_2) \\ a_{12} &= -m_3L_1L_3\sin(q_2) \\ d_{0,2} &= m_3L_3(L_2\cos(q_2) + L_1\cos(q_1 + q_2)) \\ G_0 &= -\frac{\partial V}{\partial q_0}(q) = g_0(m_1 + m_2 + m_3)L_1\cos(q_0) + g_0(m_2 + m_3)L_2\cos(q_0 + q_1) + g_0m_3L_3\cos(q_0 + q_1 + q_2),\end{aligned}\tag{46}$$

with $d_{0,0}$, $d_{0,1}$ as given in Lemma 2, (35). Note that σ is the angular momentum of the robot about the attachment point and is computed from the above data via (9).

C.2 Control Law Design

The goal is to demonstrate local exponential stability and asymptotic tracking about an equilibrium point. An equilibrium point $(q^e, 0)$ was found from $\frac{\partial V}{\partial q_0}(q)(q^e) = 0$, $q_0^e = \pi/3$, and $q_0^e + q_1^e + q_2^e = \pi/3$, resulting in $q^e = (1.0472, 1.4522, -1.4522)$; see Figure 5 (a).

The control law design consists of the preliminary feedback needed to place the system in (modified) Spong normal form (as explained in the Appendix), the selection of two outputs, the dynamic extension that renders the system statically decouplable (and hence statically input-output linearizable), and a

second static state feedback used to linearize and stabilize the input-output map. For the three-link robot, the outputs have been selected as

$$\begin{aligned} y_1 &= K p_1 + \sigma \\ y_2 &= q_2 - q_2^e, \end{aligned} \quad (47)$$

where $K > 0$ is to be chosen, and the function p_1 is determined this time via Remark 7. The dynamic extension is

$$\begin{aligned} v_1 &= w_1 \\ \dot{v}_2 &= w_2, \end{aligned} \quad (48)$$

which consists of adding a single integrator on v_2 . Introduce a state vector $x = (q_0, \sigma, q_1, \dot{q}_1, q_2, \dot{q}_2, v_2)$, and express the composition of (45), (47), and (48) as

$$\begin{aligned} \dot{x} &= f(x) + g(x)w \\ y &= h(x). \end{aligned} \quad (49)$$

Direct calculation confirms that y has (vector) relative degree three [22] with respect to w . Indeed, using Lie derivative notation, the output derivatives are

$$\begin{aligned} \dot{y} &= L_f h(x) \\ \ddot{y} &= L_f^2 h(x) \\ y^{(3)} &= L_f^3 h(x) + L_g L_f^2 h(x)w, \end{aligned} \quad (50)$$

where $L_g L_f^2 h$ corresponds to the decoupling matrix M in (21). Evaluating the right hand side of (22) at the equilibrium point gives -2.35 , and thus the decoupling matrix is invertible in a neighborhood of this point. It follows that a feedback law that provides asymptotic tracking is [22]

$$w = [L_g L_f^2 h]^{-1} \left[y_r^{(3)} - L_f^3 h + \sum_{j=0}^2 \bar{K}_j (y_r^{(j)} - L_f^j h) \right], \quad (51)$$

for any choice of constant matrices \bar{K}_j that renders the error equation exponentially stable: $e^{(3)} + \sum_{j=0}^2 \bar{K}_j e^{(j)} = 0$, for $e := (y_r - y)$.

For the simulation, the matrices \bar{K}_j were arbitrarily chosen to be diagonal and to place all of the eigenvalues of the error equation at -1 . The free parameter in the output was arbitrarily chosen as $K = 5$. Since $d_{0,0}(q^e) \approx 14.5$, the zero dynamics is about one third as fast as the output error equation.

C.3 Simulation results

The simulation demonstrates asymptotic tracking and exponential stabilization. The initial condition was taken as $(1.1, 1.42, -1.80, 0, 0, 0)$, and is depicted in Figure 5 (b). For the first forty seconds, the robot is commanded to track sinusoidal references that cause it to execute a form of calisthenics, namely, deep knee bends; at forty seconds, the references are abruptly set to constant values corresponding to the equilibrium point q^e in order to demonstrate convergence to a constant set point. The asymptotic convergence of the outputs to the commanded references is shown in Figure 6. The evolution of the configuration variables and the applied joint torques is shown in Figure 7; this same figure also shows the evolution of p_1 and $M_{1,1}$. An animation of the motion is available at [20].

D. Planar Two-Link Structure in Ballistic Motion

This examples illustrates how the locally linearizing coordinates of Theorem 2 can be used to advantage in planning a flip gait in a planar two link structure undergoing ballistic motion. The boundary constraints chosen in the flip gait are motivated by bipedal running [9]. The singularities in the decoupling matrix will be explicitly computed and related to configuration changes of the mechanism.

As shown in Figure 8, the mechanism consists of three point masses joined by two massless bars in an actuated, revolute joint. The four configuration variables are selected as q_0 , q_1 , x_c , and y_c , where q_0 relates the orientation of the mechanism to a world frame and q_1 is the relative angle between the two links. The mechanism's position with respect to a world frame is represented by the Cartesian coordinates of its center of mass. The point masses are given by m_0 , m_1 , m_2 ; the bar connecting m_0 to m_1 has length L_1 and that connecting m_1 to m_2 has length L_2 .

D.1 Mathematical representation

The complete dynamic model is easily obtained using the method of Lagrange and yields immediately the modified Spong normal form (11)

$$\begin{aligned} \dot{q}_0 &= \frac{\sigma - d_{0,1}(q_1)\dot{q}_1}{d_{0,0}(q_1)} \\ \dot{\sigma} &= 0 \\ \ddot{q}_1 &= v \\ \ddot{x}_c &= 0 \\ \ddot{y}_c &= g_0, \end{aligned} \tag{52}$$

with control v and

$$\begin{aligned} d_{0,0}(q_1) &= a_{00} + a_{01}\cos(q_1) \\ d_{0,1}(q_1) &= a_{10} + a_{11}\cos(q_1) \\ a_{00} &= \frac{m_0(m_1+m_2)L_1^2 + m_2(m_0+m_1)L_2^2}{m_0+m_1+m_2} \\ a_{01} &= 2a_{11} \\ a_{10} &= \frac{m_2(m_0+m_1)L_2^2}{m_0+m_1+m_2} \\ a_{11} &= \frac{m_0m_2L_1L_2}{m_0+m_1+m_2}. \end{aligned} \tag{53}$$

The strongly accessible portion of the model has dimension three, and involves q_0 , q_1 , \dot{q}_1 . Due to ballistic motion, there is a five dimensional uncontrollable subsystem that is completely decoupled from the actuated portion of the model, and this is given by x_c , y_c , σ , \dot{x}_c , \dot{y}_c . How these two parts interact in a path planning problem is explained next.

D.2 Interaction through boundary conditions

The flight phases of a gymnastic robot, such as a tumbler or a bipedal runner, are typically short-term motions that alternate with single support phases⁴. The creation of an overall satisfactory motion is closely tied to achieving correct boundary conditions at the interfaces of the flight and single support

⁴That is, one end of the mechanism is in contact with a rigid surface, and the contact point is neither slipping nor rebounding; in other words the contact point is acting as a pivot.

phases. The state of the robot at the end of a flight phase determines the initial conditions for the single support phase, and consequently the state of the robot at the end of a flight phase is typically more important than the exact trajectory followed during the flight phase.

At the beginning and end of a flight phase, the robot is in contact with a surface, assumed here to be identified with the horizontal component of the world frame. Assume furthermore that the robot is in single support, with the contact point being either the mass m_0 or m_2 . In single support, there are two holonomic constraints that tie the position and velocity of the center of mass to those of the angular coordinates; in other words, there is a loss of two degrees of freedom. Conservation of angular momentum through $\dot{\sigma} = 0$ yields an additional (nonholonomic) constraint on the angular velocities. In particular, the desired final joint velocities must be chosen to satisfy this constraint.

The duration of the flight phase, T , is determined from $\ddot{y}_c = g_0$, with the initial conditions coming from the initial positions and velocities of the angular coordinates at lift-off, and the end condition of the height of the center mass coming from the desired final configuration of the angular coordinates at touch-down. Once the flight time is known, determining whether or not there exists a solution of the reduced model,

$$\begin{aligned}\dot{q}_0 &= \frac{\sigma - d_{0,1}(q_1)\dot{q}_1}{d_{0,0}(q_1)} \\ \ddot{q}_1 &= v,\end{aligned}\tag{54}$$

that is compatible with a given set of initial and final conditions is a difficult problem: once a trajectory for $q_1(t)$ is chosen, \dot{q}_0 must be numerically integrated, and if $q_0(T)$ does not have the desired value, then $q_1(t)$ must be altered. Such an iterative procedure is poorly adapted to on-line computations. Theorem 2 will be applied to simplify this task. It should be noted that the value of the momentum σ is unknown before the start of the flight phase, and thus it is not even possible to determine the reduced model (54) before the initial condition of the robot is known at lift-off.

D.3 Determining a ballistic motion trajectory in linearizing coordinates

Local, input-output linearizing coordinates for the reduced model (54) are constructed from $y = p_1$ and its first two derivatives. Define p_1 by (41). Direct computation leads to

$$\dot{p}_1 = \frac{\sigma}{d_{0,0}(q_1)} = \frac{\sigma}{a_{00} + a_{01} \cos(q_1)}\tag{55}$$

$$\ddot{p}_1 = \frac{\sigma \frac{d}{dq_1} d_{0,0}(q_1)}{d_{0,0}(q_1)^2} \dot{q}_1 = \frac{\sigma a_{01} \sin(q_1)}{(a_{00} + a_{01} \cos(q_1))^2} \dot{q}_1.\tag{56}$$

To determine the linearizing control, one more derivative is needed

$$p_1^{(3)} = \sigma a_{01} \frac{(2a_{01} + a_{00} \cos(q_1) - a_{01} \cos^2(q_1))}{(a_{00} + a_{01} \cos(q_1))^3} \dot{q}_1^2 + M_{1,1} v\tag{57}$$

$$M_{1,1} = \frac{\sigma \frac{d}{dq_1} d_{0,0}(q_1)}{d_{0,0}(q_1)^2} = \frac{\sigma a_{01} \sin(q_1)}{(a_{00} + a_{01} \cos(q_1))^2}.\tag{58}$$

Wherever $M_{1,1} \neq 0$, a linearizing feedback can be constructed such that

$$p_1^{(3)} = w. \quad (59)$$

For arbitrary initial and final conditions of the linear model (59), it is trivial to define a feasible trajectory. Indeed, it suffices to define a three-times continuously differentiable function passing from given initial values to given final values. One could even use a polynomial of order five or greater.

Since the change of coordinates going from (54) to (59) is local, not every solution of (59) can be mapped back onto a solution of (54). From (55), p_1 , the ‘‘global’’ orientation of the robot, can only be changed through modification of the inertia parameter, $d_{0,0}$, because the angular momentum is constant. The inertia term $d_{0,0}$ can only be changed through variation of the internal angle, q_1 . Since $d_{0,0}$ is bounded, so is \dot{p}_1 . These kinds of constraints, which must be applied point-wise in time on the trajectories of (59), are made explicit by computing the inverse of the coordinate change.

D.4 Constraints point-wise in time associated with the linearizing coordinates

The calculation of q_0, q_1, \dot{q}_1 in terms of $p_1, \dot{p}_1, \ddot{p}_1$ yields

$$q_1 = \arccos\left(\frac{\frac{\sigma}{\dot{p}_1} - a_{00}}{a_{01}}\right) \quad (60)$$

$$q_0 = p_1 - \frac{a_{11}}{a_{01}}q_1 - 2 \left(\frac{a_{10}}{\sqrt{a_{00}^2 - a_{01}^2}} - \frac{a_{00}a_{11}}{a_{01}\sqrt{a_{00}^2 - a_{01}^2}} \right) \arctan \left(\frac{a_{00} - a_{11}}{\sqrt{a_{00}^2 - a_{01}^2}} \tan\left(\frac{q_1}{2}\right) \right) \quad (61)$$

$$\dot{q}_1 = \frac{\ddot{p}_1(a_{00} + a_{01} \cos(q_1))^2}{\sigma a_{01} \sin(q_1)} \quad (62)$$

The first equation only admits a solution for $\frac{\sigma}{a_{00}-a_{01}} \leq \dot{p}_1 \leq \frac{\sigma}{a_{00}+a_{01}}$, and then has two solutions: one for $0 \leq q_1 < \pi$ and another for $-\pi \leq q_1 < 0$. These two domains for the cosine define two ‘‘configuration classes’’ of the robot, with the extreme points of the domains corresponding to the links being completely folded or unfolded. At the extreme points of the domains, \dot{p}_1 attains an extremum and consequently, \ddot{p}_1 is zero. At an extreme point of q_1 , \dot{q}_1 cannot be determined from (62), which takes the form $\dot{q}_1 = \frac{0}{0}$. Since $M_{1,1}$ vanishes at an extreme point, (57) is used with $M_{1,1} = 0$ to obtain

$$\dot{q}_1 = \pm \sqrt{\frac{p_1^{(3)} (a_{00} + a_{01} \cos(q_1))^3}{\sigma a_{01} (2a_{01} - a_{01} \cos^2(q_1) + a_{00} \cos(q_1))}}, \quad (63)$$

with the sign of \dot{q}_1 being determined by continuity (with torque control, there cannot be discontinuities in the velocity). The robot will then pass through the singularity, and change configuration classes.

Consequently, when generating a motion, two cases can present themselves, according to whether the motion stays always in the same configuration class or not. If the initial and final configuration are in the same configuration class, then a trajectory can be generated by imposing $\frac{\sigma}{a_{00}-a_{01}} < \dot{p}_1(t) < \frac{\sigma}{a_{00}+a_{01}}$. Both open-loop and feedback controls are equally easily computed starting from the linear model. If

the initial and final configurations are in different configuration classes, a trajectory can be computed that passes through a singularity at a single time instance, $0 \leq t_0 \leq T$, where $M_{1,1}$ vanishes. An open-loop control can be determined as before. On the other hand, a feedback implementation is not possible based on inverting $M_{1,1}$ in (58). However, since the flight phase is typically of short duration and the input is calculated as a function of the initial conditions, an open-loop control is probably sufficient.

D.5 Simulation without passing through a singularity

The model parameters were selected as $L_1 = 1.0$, $L_2 = 1.0$, $m_0 = 1.0$, $m_1 = 2.0$, $m_2 = 1.0$. For this simulation, the mass m_0 of the robot is supposed initially in contact with the ground, with configuration defined by $q_0 = 3\pi/4$, $q_1 = -\pi/4$, and angular velocities $\dot{q}_0 = -5$, $\dot{q}_1 = 0$. The objective is to transfer the robot at the end of a flight phase so that when the mass m_2 of the robot touches the ground, its configuration is $q_0 = -0.5$, $q_1 = -\pi/4$ with angular velocity proportional to $\dot{q}_0 = 1$, $\dot{q}_1 = 0$. The initial and final configurations are depicted in Figure (9); they belong to the same configuration class. From the initial conditions of the robot and the desired final configuration, the flight time is computed as $T = 0.5173$. Conservation of angular momentum implies that $\dot{q}_0(T) = -5$.

The initial and final values of p_1 and its first two derivatives were computed from (41), (55), and (56). A fifth-order polynomial of t was defined that satisfied these boundary conditions. The resulting trajectories of $p_1, \dot{p}_1, \ddot{p}_1$ are depicted in Figure 10; the point-wise in time constraints associated with (60), (61) and (62) are met. The input torque u for the system was computed using (57) and (75) of the Appendix. The resulting trajectories in terms of q and \dot{q} are shown in Figure 11 and the evolution of the robot in the vertical plane is presented in Figure 9. An animation of the motion is available at [20].

D.6 Simulation with passage through a singularity

For this simulation, the mass m_0 of the robot is supposed initially in contact with the ground, with configuration defined by $q_0 = 3\pi/4$, $q_1 = \pi/4$ and angular velocities $\dot{q}_0 = -5$, $\dot{q}_1 = 0$. The objective is to transfer the robot at the end of a flight phase so that when the mass m_2 of the robot touches the ground, its configuration is $q_0 = -0.5$, $q_1 = -\pi/4$ with angular velocity proportional to $\dot{q}_0 = 0$, $\dot{q}_1 = 1$. The initial and final configurations are depicted in Figure (12); they do not belong to the same configuration class. From the initial conditions of the robot and the desired final configuration, the flight time is computed as $T = 0.7062s$. Conservation of angular momentum implies that $\dot{q}_0(T) = -5$.

The initial and final values of p_1 and its first two derivatives were computed as before. So that the robot changes configuration class, at $t_s = T/2$, the trajectory was forced to pass through a singularity corresponding to $q_1 = 0$, that is, $\ddot{p}_1 = 0$ and $\dot{p}_1 = \sigma/(a_{00} + a_{01})$. A seventh-order polynomial in t was defined that satisfied the six boundary conditions, plus $\ddot{p}_1(t_s) = 0$, $\dot{p}_1(t_s) = \sigma/(a_{00} + a_{01})$. The

resulting trajectories of $p_1, \dot{p}_1, \ddot{p}_1$ are depicted in Figure 13. The corresponding trajectories in terms of q and \dot{q} are shown in Figure 14 and the evolution of the robot in the plane is presented in Figure 12. An animation of the motion is available at [20].

V. ADDITIONAL TECHNICAL POINTS

This section provides additional discussion on a few points that would have broken the flow of the main developments.

A. A cascade structure

The feedback designs of Section III-C that have been illustrated on the two-link and three-link models have singularities where the decoupling matrix loses rank. Results in [21] show that (within the category of analytic systems and compensators) achieving an invertible decoupling matrix via dynamic compensation is a necessary condition for the existence of a compensator that achieves asymptotic tracking of an open set of reference trajectories. Hence, while it is not necessary that the particular decoupling matrix constructed in (21) be invertible, at least some other decoupling matrix would have to be invertible for asymptotic tracking to be possible on a larger set.

If one is only trying to accomplish stabilization on a large set and not asymptotic tracking, it is then interesting to consider feedback designs that avoid the requirement of an invertible decoupling matrix. One way that this may be approached for the systems studied in Section III-C is the following. First, use (13) to rewrite (11) in the coordinates $(p_1, \sigma, q_1, \dots, q_{N-1}, \dot{q}_1 \dots \dot{q}_{N-1})$ as

$$\begin{aligned} \dot{p}_1 &= \frac{\sigma}{d_{0,0}(q_1, \dots, q_{N-1})} + \sum_{k=2}^{N-1} J_k(q_1, \dots, q_{N-1}) \dot{q}_k \\ \dot{\sigma} &= \bar{G}_0(p_1, q_1, \dots, q_{N-1}) \\ \ddot{q}_j &= v_j \quad j = 1, \dots, N-1, \end{aligned} \quad (64)$$

where

$$\bar{G}_0(p_1, q_1, \dots, q_{N-1}) := - \frac{\partial V}{\partial q_0}(q_0, q_1, \dots, q_{N-1}) \Bigg|_{q_0 = p_1 + q_0^e - \int_{q_1^e}^{q_1} \frac{d_{0,1}}{d_{0,0}}(\tau, q_2, \dots, q_{N-1}) d\tau}. \quad (65)$$

Define $x_1 = (p_1, \sigma)'$, $x_2 = q_1$, $x_3 = \dot{q}_1$, $x_4 = (q_2, \dots, q_{N-1})'$, $x_5 = (\dot{q}_2, \dots, \dot{q}_{N-1})'$, $\bar{v}_1 = v_1$ and $\bar{v}_2 = (v_2, \dots, v_{N-1})'$. Then (64) takes the form of a feedforward nonlinear system

$$\begin{aligned} \dot{x}_1 &= f_1(x_1, x_2, x_4) + g_1(x_2, x_4)x_5 \\ \dot{x}_2 &= x_3 \\ \dot{x}_3 &= \bar{v}_1 \\ \dot{x}_4 &= x_5 \\ \dot{x}_5 &= \bar{v}_2, \end{aligned} \quad (66)$$

for which various feedback stabilization methods have been developed [51], [45], [44], [27]. Backstepping suggests considering x_2 and x_5 as virtual controls [25], leading to the simpler (block-)feedforward system

$$\begin{aligned} \dot{x}_1 &= f_1(x_1, x_2, x_4) + g_1(x_2, x_4)x_5 \\ \dot{x}_4 &= x_5. \end{aligned} \quad (67)$$

For a two-link system, x_4 and x_5 are empty, leading to the two dimensional system $\dot{x}_1 = f_1(x_1, x_2)$, the global asymptotic stabilization⁵ of which has been studied in [33]. The problem of asymptotically stabilizing (67) on large sets is open for systems with three or more links.

B. Checking feedback linearizability

This subsection offers a few observations on the generic non-feedback linearizability of the model class studied here when generalized conjugate momentum is not conserved. The reason to check this property is that if the systems were feedback linearizable, then it always would be possible to achieve an empty zero dynamics instead of one with dimension one. Recall that for single-input systems, it is known that a system is dynamically feedback linearizable if, and only if, it is statically feedback linearizable. For multi-input systems, dynamic feedback does enlarge the class of linearizable systems, but necessary and sufficient conditions for dynamic feedback linearizability are not known. If one restricts the outputs used to achieve dynamic feedback linearizability (often called flat outputs) to being only functions of the configuration variables, however, then for mechanical systems with one degree of underactuation, necessary and sufficient conditions for dynamic feedback linearization are known [39]; in particular, for the class of systems being studied in this paper, the conclusion is that there do not generally exist flat outputs depending only on the configuration variables.

Consider first a 2-DOF system written in the form of (64), and suppose that $\bar{G}_0 \neq 0$. Such a system has a single input and thus necessary and sufficient conditions for feedback linearizability can be checked. Applying the method of [12], the system is feedback linearizable if, and only if,

- either $\frac{d}{dq_1}(d_{0,0}) \equiv 0$, in which case p_1 is a linearizing (or flat) output,
- or, $\frac{d}{dq_1}(d_{0,0}) \not\equiv 0$ and $\frac{d}{dq_1}(\beta) \equiv 0$, where $\beta = \left(\frac{d_{0,0}^2}{\frac{d}{dq_1}(d_{0,0})} \frac{\partial \bar{G}_0}{\partial q_1} \right)$, in which case $\sigma^2 + 2\beta p_1$ is a linearizing (or flat) output.

These conditions are not generally satisfied for the class of systems being studied; in particular, applying them to the two link example of Section IV-B proves that it is not feedback linearizable.

Consider next a system with 3-DOF written either in the form (11) or (64). Applying once again the method in [12], the system is statically feedback linearizable only if

$$\frac{\partial J_2}{\partial q_1} \equiv 0; \quad (68)$$

moreover, the same obstruction persists if an integrator is added on v_2 so the dynamic extension used in the paper does not render the system static feedback linearizable. The obstruction (68) is present in the three link example of Section IV-C.

The only example known at this time to be feedback linearizable is the inertia wheel pendulum [50], which satisfies the condition $\frac{d}{dq_1}(d_{0,0}) \equiv 0$, and thus p_1 is a linearizing output. The method of this

⁵The Lyapunov function used in [33] was not shown to be proper or radially unbounded. For the Acrobot, a periodicity property of \bar{G}_0 can be used to fill this lacuna when the dynamic model is extended in the obvious way to \mathbb{R}^4 .

paper also finds locally linearizing coordinates. In the coordinates of Figure 1, the modified Spong normal form of the inertia wheel pendulum is

$$\begin{aligned}\dot{q}_0 &= \frac{\sigma}{d_{0,0}} - \frac{d_{0,1}}{d_{0,0}}\dot{q}_1 \\ \dot{\sigma} &= G_0 \\ \ddot{q}_1 &= v_1,\end{aligned}\tag{69}$$

where

$$\begin{aligned}d_{0,0} &= m_1 l_{c1}^2 + m_2 l_1^2 + I_1 + I_2 \\ d_{0,1} &= I_1 \\ G_0 &= \bar{m} g_0 \cos(q_0) \\ \bar{m} &= m_1 l_{c1} + m_2 l_1,\end{aligned}\tag{70}$$

and the parameters are as defined in [50]. Since $d_{0,0}$ and $d_{0,1}$ are constant, (6) is trivially integrated about the equilibrium point $q^e = (\pi/2, 0, 0, 0)$ to obtain

$$p_1 = (q_0 - \pi/2) + \frac{d_{0,1}}{d_{0,0}} q_1.\tag{71}$$

Defining the output as $y = Kp_1 + \sigma$ and using (13) and (17)-(19), the model (69) in the coordinates $(x_1, x_2, x_3, x_4) = (y, \dot{y}, \ddot{y}, p_1)$ becomes

$$\begin{aligned}\dot{x}_1 &= x_2 \\ \dot{x}_2 &= x_3 \\ \dot{x}_3 &= * + M_{1,1} v_1 \\ \dot{x}_4 &= \frac{1}{d_{0,0}} x_1 - \frac{K}{d_{0,0}} x_4.\end{aligned}\tag{72}$$

At the upright equilibrium, $M_{1,1} = \bar{m} g_0 \frac{d_{0,1}}{d_{0,0}} \neq 0$, and hence (72) is linear in the coordinates (x_1, x_2, x_3, x_4) after the application of a static state feedback.

Remark 8: More generally, the underlying reason for the static feedback linearizability of the inertia wheel pendulum can be tied to be the following result, which applies to N DOF mechanisms (2). Consider again the one-form $\omega = \sum_{k=0}^{N-1} d_{0,k}(q_1, \dots, q_{N-1}) dq_k$ associated with the generalized conjugate momentum (9) and suppose that ω is closed. Let $d\theta = \omega$. Then a simple computation shows that: (a) θ has at least relative degree four; (b) the outputs $y_1 = \theta(q) - \theta(q^e)$, $y_i = q_i - q_i^e$, $i = 2, \dots, N-1$ have decoupling matrix (21) with $K = 0$; (c) when the decoupling matrix is invertible, these outputs have vector relative degree $(4, 2, \dots, 2)$ and thus the system is static feedback linearizable; and (d) the coordinate transformation required to linearize the system is canonical and given by $\bar{q} = \Phi(q)$, $\dot{\bar{q}} = \frac{\partial \Phi}{\partial q} \dot{q}$, where $\Phi(q) = (y_1, -\frac{\partial V}{\partial q_0}, y_2, \dots, y_{N-1})'$. For the inertia wheel pendulum ω is closed because the first row of the inertia matrix is constant; moreover, the relative degree four function θ is proportional to p_1 .

VI. CONCLUSIONS

Motivated by a large number of dexterous robots that have been introduced in the literature over the past fifteen years, this paper has analyzed simple planar mechanical systems with an unactuated

cyclic variable and an independent actuator for each shape variable. This class of models is naturally associated with balancing tasks and includes N -link extensions of the Acrobot, the stance phase of Raibert's hopper and many other robots. Typical control objectives include stabilizing an equilibrium and asymptotically tracking a pre-defined motion. Through a simple decomposition procedure, models with an unactuated cyclic variable and an independent actuator for each shape variable also arise for certain systems executing a ballistic motion, such as diving, dismounting from a highbar, and tumbling. For these systems, since momentum is conserved, since the initial conditions are usually determined by the end of a single support phase, and since the ballistic phase is usually of short duration, asymptotically tracking a pre-defined motion is not a reasonable objective. Instead, the main problem is to determine if a set of initial and final conditions is compatible, and if so, to generate on-line a trajectory that joins them.

The paper presented two novel control results. When the generalized momentum conjugate to the cyclic variable was not conserved, conditions were found for the existence of a set of outputs that yielded a one-dimensional, exponentially stable zero dynamics, along with a dynamic extension that rendered the system locally input-output decouplable. By existing results, a controller that achieves asymptotic stabilization and tracking is then easily constructed. When the generalized momentum conjugate to the cyclic variable was conserved, a reduced system was constructed and conditions were found for the existence of a set of outputs that yielded an empty zero dynamics, along with a dynamic extension that rendered the system locally input-output decouplable. By existing results, a local coordinate transformation and dynamic feedback controller that linearize the input-to-state map are then easily constructed. The solutions to these two control problems had a common underlying element: the computation of a function of the configuration variables that had relative degree three with respect to one of the input components after an appropriate static feedback. It was interesting that this function arose by partially integrating a physical quantity, the conjugate momentum.

The theoretical results were illustrated on three simple examples. Stabilization of an equilibrium was demonstrated on a variant of the Acrobot without the influence of gravity. The purpose of the example was to emphasize the role of the potential energy in determining whether generalized momentum is conserved, and to demonstrate the computations needed to apply the results of the paper in the simplest possible setting. Asymptotic stabilization about an equilibrium and asymptotic tracking were both illustrated on a serial, three-link, mechanism attached to a pivot and constrained to evolve in a vertical plane. This example provided a non-trivial illustration of the results for a system with multiple inputs. The last example illustrated how locally linearizing coordinates can simplify the path planning problem for a ballistic flip motion of a two-link mechanism. The singularities in the decoupling matrix were explicitly computed and related to configuration changes of the mechanism.

ACKNOWLEDGMENTS

The work of J.W. Grizzle was supported by NSF grant ECS-0322395.

VII. APPENDIX

Spong Normal Form:

The Spong normal form is taken from [49], [40]. Let $F(q, \dot{q}) := C(q, \dot{q})\dot{q} + G$ and partition the generalized coordinates into actuated and unactuated parts per $q = (q_0, \bar{q}_1)$, $\bar{q}_1 = (q_1, \dots, q_{N-1})$. This induces a decomposition of the model (2)

$$\begin{aligned} d_{0,0}\ddot{q}_0 + D_{0,1}\ddot{\bar{q}}_1 + F_0 &= 0 \\ D_{1,0}\ddot{q}_0 + D_{1,1}\ddot{\bar{q}}_1 + F_1 &= u. \end{aligned} \quad (73)$$

Define

$$\begin{aligned} \bar{D} &= D_{1,1} - D_{1,0}D_{0,1}/d_{0,0} \\ \bar{F} &= F_1 - D_{1,0}F_0/d_{0,0} \\ R &= -F_0/d_{0,0}. \end{aligned} \quad (74)$$

The static state feedback taking (2) into (8) is

$$u = \bar{D}v + \bar{F}. \quad (75)$$

The feedback is regular because $(\det \bar{D})d_{0,0} = \det D$ and $d_{0,0} \neq 0$.

Parameterization of the zero dynamics:

From the choice of outputs (15), $dy_k^{(j)} = dq_k^{(j)}$, $j = 0, 1, 2$; $2 \leq k \leq N - 1$. Hence, to determine the zero dynamics, it is enough to find a function whose differential is independent of $\{dy_1^{(j)}, j = 0, 1, 2\}$, modulo

$$\text{span}\{dq_k^{(j)}, j = 0, 1, 2; 2 \leq k \leq N - 1\}. \quad (76)$$

This is most easily done if the model is expressed in the coordinates $\tilde{q} := (p_1, q_1, \dots, q_n)$. Then, the condition (22) for the invertibility of the decoupling matrix at an equilibrium becomes

$$\left. \frac{\partial^2 \tilde{V}}{\partial q_1 \partial p_1} \right|_{\tilde{q}^e} \neq 0, \quad (77)$$

where, in the new coordinates, \tilde{q}^e is the equilibrium point and the potential energy is

$$\tilde{V}(p_1, q_1, \dots, q_n) = V(q_0, q_1, \dots, q_n) \Big|_{q_0=p_1 - \int_{q_1^e}^{q_1} \frac{d_{0,1}}{d_{0,0}}(\tau, q_2, \dots, q_{N-1}) d\tau}.$$

The model (8) with the dynamic extension (16) can be rewritten as

$$\begin{aligned} \dot{p}_1 &= \frac{\sigma}{d_{0,0}(q_1, \dots, q_{N-1})} + \sum_{k=2}^{N-1} \beta_k(q_1, \dots, q_{N-1}) \dot{q}_k \\ \dot{\sigma} &= -\frac{\partial \tilde{V}}{\partial p_1}(p_1, q_1, \dots, q_{N-1}) \\ \ddot{q}_1 &= w_1 \\ q_k^{(3)} &= w_k, \quad 2 \leq k \leq N - 1. \end{aligned} \quad (78)$$

Computing (y_1, \dot{y}_1) and evaluating their differentials at the equilibrium point and modulo (76), results in

$$\begin{aligned} dy_1 &= K dp_1 + d\sigma \\ d\dot{y}_1 &= \frac{K}{d_{0,0}} d\sigma - \frac{\partial^2 \tilde{V}}{\partial p_1^2} dp_1 - \frac{\partial^2 \tilde{V}}{\partial q_1 \partial p_1} dq_1 \end{aligned} \quad (79)$$

and hence $\text{span}\{dp_1, dy_1, d\dot{y}_1\} = \text{span}\{dp_1, d\sigma, dq_1\}$ modulo (76). Next, computing \ddot{y}_1 and evaluating its differential at the equilibrium point and modulo (76) and $\text{span}\{dp_1, d\sigma, dq_1, \}$ yields

$$d\ddot{y}_1 = -\frac{\partial^2 \tilde{V}}{\partial q_1 \partial p_1} d\dot{q}_1, \quad (80)$$

and thus, $\text{span}\{dp_1, dy_1, d\dot{y}_1, d\ddot{y}_1\} = \text{span}\{dp_1, d\sigma, dq_1, d\dot{q}_1\}$ modulo (76), proving that p_1 can be used to parameterize the zero dynamics in a neighborhood of an equilibrium point.

REFERENCES

- [1] M. Ahmadi and M. Buehler. Stable control of a simulated one-legged running robot with hip and leg compliance. *IEEE Transactions on Robotics and Automation*, 13(1):96–104, February 1997.
- [2] M.D. Berkemeier and R.S. Fearing. Tracking fast inverted trajectories of the underactuated acrobot. *IEEE Transactions on Robotics and Automation*, 15(4):740–750, August 1999.
- [3] A.M. Bloch, N.E. Leonard, and J.E. Marsden. Controlled lagrangians and the stabilization of mechanical systems. I: The first matching theorem. *IEEE Transactions on Automatic Control*, 45(12):2253–2270, December 2000.
- [4] F. Bullo and K. M. Lynch. Kinematic controllability for decoupled trajectory planning in underactuated mechanical systems. *IEEE Transactions on Robotics and Automation*, 17(4):402–412, August 2001.
- [5] L. Cambrini, C. Chevallereau, C.H. Moog, and R. Stojic. Stable trajectory tracking for biped robots. In IEEE Press, editor, *Proceedings of the 39th IEEE Conference on Decision and Control, Sydney, Australia*, pages 4815–4820, December 2000.
- [6] C. Canudas-de-Wit, L. Rousset, and A. Goswami. Periodic stabilization of a 1-DOF hopping robot on nonlinear compliant surface. In *Proc. of IFAC Symposium on Robot Control, Nantes, France*, pages 405–410, September 1997.
- [7] C. Chevallereau. Robotics team at IRCCyN. <http://www.ircyn.ec-nantes.fr/ircyn/d/en/equipements/Robotique/Membres>, April 2003.
- [8] C. Chevallereau, G. Abba, Y. Aoustin, F. Plestan, E.R. Westervelt, C. Canudas-de Wit, and J.W. Grizzle. RABBIT: A testbed for advanced control theory. *IEEE Control Systems Magazine*, 23(5):57–79, October 2003.
- [9] C. Chevallereau and Y. Aoustin. Optimal reference trajectories for walking and running of a biped robot. *Robotica*, 19(5):557–569, September 2001.
- [10] C. Chevallereau, A. Formal'sky, and D. Djoudi. Tracking of a joint path for the walking of an underactuated biped. *Robotica*, 2003. accepted for publication; pre-print available at [7].
- [11] C. Chevallereau and P. Sardain. Design and actuation optimization of a 4 axes biped robot for walking and running. In *Proc. of the IEEE International Conference on Robotics and Automation, San Francisco, California*, pages 3365–3370, April 2000.
- [12] G. Conte, C.H. Moog, and A.M. Perdon. *Nonlinear Control Systems : An Algebraic Setting*, volume 242 of *Lecture Notes in Control and Information Science*. Springer Verlag, March 1999.
- [13] M. Fliess, J. Lévine, P. Martin, and P. Rouchon. Flatness and defect of non-linear systems: introductory theory and examples. *International Journal of Control*, 61:pp. 1327–1361, 1995.
- [14] M. Fliess, J. Levine, P. Martin, and P. Rouchon. A lie-backlund approach to equivalence and flatness of nonlinear systems. *TAC*, 44(5):922–937, May 1999.
- [15] C. Francois and C. Samson. A new approach to the control of the planar one-legged hopper. *International Journal of Robotics Research*, 17(11):1150–1166, 1998.
- [16] T. Fukuda and F. Saito. Motion control of a brachiation robot. *Robotics and Autonomous Systems*, 18:83–93, July 1996.
- [17] T. Geng and X. Xu. Flip gait synthesis of a biped based on poicare map. In *Proc. of the Second International Workshop On Robot Motion And Control, Bukoway Dworek, Poland*, pages 239–243. IEEE Robotics and Automation Society, October 2001.
- [18] J.M. Godhavn, A. Balluchi, L. Crawford, and S. Sastry. Path planning for nonholonomic systems with drift. In *Proc. of the American Control Conference, Albuquerque, NM*, pages 532–536, June 1997.
- [19] H. Goldstein. *Classical Mechanics*. Addison Wesley, second edition, 1980.
- [20] J.W. Grizzle. Publications on robotics and control. <http://www.eecs.umich.edu/~grizzle/papers/robotics.html>, September 2003.
- [21] J.W. Grizzle, M.D. Di Benedetto, and F. Lamnabhi-Lagarrigue. Necessary conditions for asymptotic tracking in nonlinear systems. *IEEE Transactions on Automatic Control*, 39(9):1782–1794, September 1994.
- [22] A. Isidori. *Nonlinear Control Systems: An Introduction*. Springer-Verlag, Berlin, third edition, 1995.
- [23] D.E. Koditschek and M. Buehler. Analysis of a simplified hopping robot. *International Journal of Robotics Research*, 10(6):587–605, 1991.
- [24] I. Kolmanovsky, N.H. McClamroch, and V.T. Coppola. New results on control of multibody systems which conserve angular momentum. *Journal of Dynamical and Control Systems*, 1(4):447–462, 1995.
- [25] M. Krstic, I. Kanellakopoulos, and P. Kokotovic. *Nonlinear and Adaptive Control Design*. Adaptive and Learning Systems for Signal Processing, Communications and Control. Wiley, New York, 1995.
- [26] H.G. Lee, Y.M. Kim, and H.T. Jeon. On the linearization via a restricted class of dynamic feedback. *TAC*, 45(7):1385–1391, July 2000.

- [27] J. Mareczek, M. Buss, and M. Spong. Invariance control for a class of cascade nonlinear systems. *IEEE Transactions on Automatic Control*, 47(4):1636–640, April 2002.
- [28] R. Marino. On the largest feedback linearizable subsystem. *Systems and Control Letters*, 7:pp. 345–351, 1986.
- [29] M. Miyazaki, M. Sampei, and M. Koga. Control of a motion of an acrobot approaching a horizontal bar. *Advanced Robotics*, 15(4):467–480, 2001.
- [30] M. Miyazaki, M. Sampei, M. Koga, and A. Takahashi. A control of underactuated hopping gait systems: Acrobot example. In *IEEE Conf. on Decision and Control, Sydney Australia*, pages 4797–4803, December 2000.
- [31] J. Nakanishi, T. Fukuda, and D.E. Koditschek. Preliminary studies of a second generation brachiation robot controller. In *Proc. of the IEEE International Conference on Robotics and Automation, Albuquerque, N.M.*, pages 2050–2056, April 1997.
- [32] J. Nakanishi, T. Fukuda, and D.E. Koditschek. A brachiating robot controller. *IEEE Transactions on Robotics and Automation*, 16(2):109–123, April 2000.
- [33] R. Olfati-Saber. Control of underactuated mechanical systems with two degrees of freedom and symmetry. In *Proc. of the American Control Conference at Chicago, IL*, pages 4092–4096, June 2000.
- [34] R. Olfati-Saber. Normal forms for underactuated mechanical systems with symmetry. *IEEE Transactions on Automatic Control*, 47(2):305–308, 2002.
- [35] K. Ono, K. Yamamoto, and A. Imadu. Control of giant swing motion of a two-link horizontal bar gymnast robot. *Advanced Robotics*, 15(4):449–465, 2001.
- [36] R. Ortega, M.W. Spong, and F. Gomez-Estern. Stabilization of underactuated mechanical systems via interconnection and damping assignment. *IEEE Transactions on Automatic Control*, 47(8):1281–1233, August 2002.
- [37] F. Plestan, J.W. Grizzle, E.R. Westervelt, and G. Abba. Stable walking of a 7-DOF biped robot. *IEEE Transactions on Robotics and Automation*, 19(4):653–668, August 2003.
- [38] M. Raibert. *Legged robots that balance*. MIT Press, Mass., 1986.
- [39] M. Rathinam and R.M. Murray. Configuration flatness of lagrangian systems underactuated by one control. *SIAM J. Control and Optimization*, 37(1):164–179, 1998.
- [40] M. Reyhanoglu, A. van der Schaft, N.H. McClamroch, and I. Kolmanovsky. Dynamics and control of a class of underactuated mechanical systems. *IEEE Transactions on Automatic Control*, 44(9):1663–1671, 1999.
- [41] P. Rouchon, M. Fliess, J. Levine, and P. Martin. Flatness, motion planning and trailer systems. In *Proceedings of the 32nd IEEE Conference on Decision and Control*, pages 2700–2705. IEEE, December 1993.
- [42] F. Saito, T. Fukuda, and F. Arai. Swing and locomotion control for a two-link brachiation robot. *IEEE Control Systems Magazine*, 14(1):5–12, February 1994.
- [43] M. Sampei, H. Kiyota, and M. Ishikawa. Control strategies for mechanical systems with various constraints—control of nonholonomic systems. In *IEEE Conf. on Systems, Man, and Cybernetics, III*, pages 158–167, 1999.
- [44] R. Sepulchre, M. Arcak, and A. Teel. Trading the stability of finite zeros for global stabilization of nonlinear cascade systems. *IEEE Transactions on Automatic Control*, 47(3):521–525, March 2002.
- [45] R. Sepulchre, M. Jankovic, and P. Kokotovic. *Constructive Nonlinear Control*. Communications and Control Engineering. Springer Verlag, London, 1997.
- [46] D. Seto and J. Baillieul. Control problems in super-articulated mechanical systems. *IEEE Transactions on Automatic Control*, 39(12):2442–2453, December 1994.
- [47] A. Shiriaev and C. Canudas-de-Wit. Virtual constraints: a constructive tool for orbital stabilization of underactuated nonlinear systems. *Personal Communication*, September 2003.
- [48] M.W. Spong. The swing up control problem for the acrobot. *IEEE Control Systems Magazine*, 15(1):49–55, February 1995.
- [49] M.W. Spong. Energy based control of a class of underactuated mechanical systems. In *Proc. of IFAC World Congress, San Francisco, CA*, pages 431–435, 1996.
- [50] M.W. Spong, P. Corke, and R. Lozano. Nonlinear control of the inertia wheel pendulum. *Automatica*, 37:1845–1851, 2001.
- [51] A. Teel. A nonlinear small gain theorem for the analysis of control systems with saturation. *IEEE Transactions on Automatic Control*, 41(9):1256–1270, September 1996.
- [52] E. Westervelt, J.W. Grizzle, and D.E. Koditschek. Hybrid zero dynamics of planar biped walkers. *IEEE Transactions on Automatic Control*, 48(1):42–56, January 2003.
- [53] M. Yamakita, T. Yonemura, Y. Michitsuji, and Z. Luo. Stabilization of acrobot in upright position on a horizontal bar. In *Proc. of the IEEE International Conference on Robotics and Automation, Washington, DC*, pages 3093–3098, May 2002.

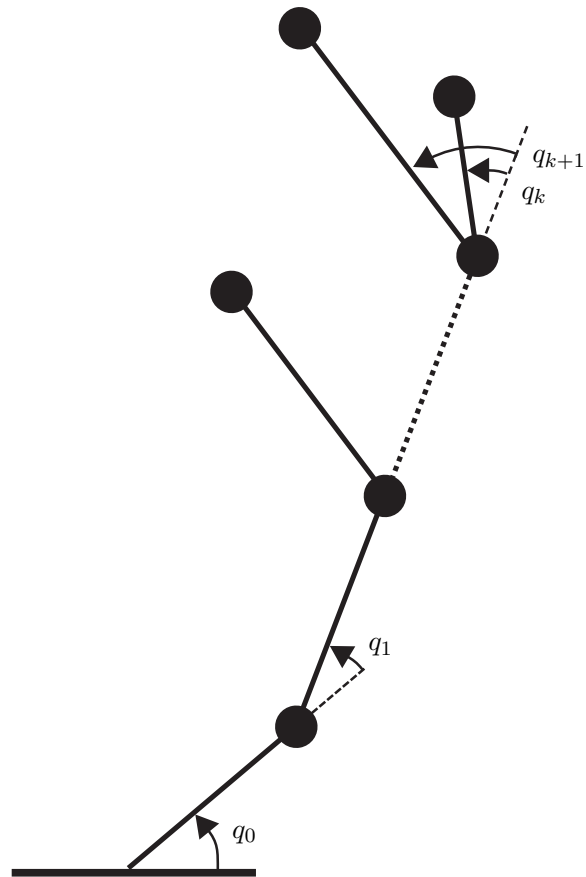


Fig. 1. A planar tree structure attached to an inertial frame via a freely acting pivot. All joints are actuated except the attachment at the pivot. A coordinate convention is indicated. Though not shown, prismatic joints and springs can also be included.

	Link 1	Link 2	Link 3
length (m)	0.4	0.4	0.3
mass (kg)	6.4	13.6	12.0

TABLE I
MASS AND LENGTH PARAMETERS FOR THREE-LINK MECHANISM.

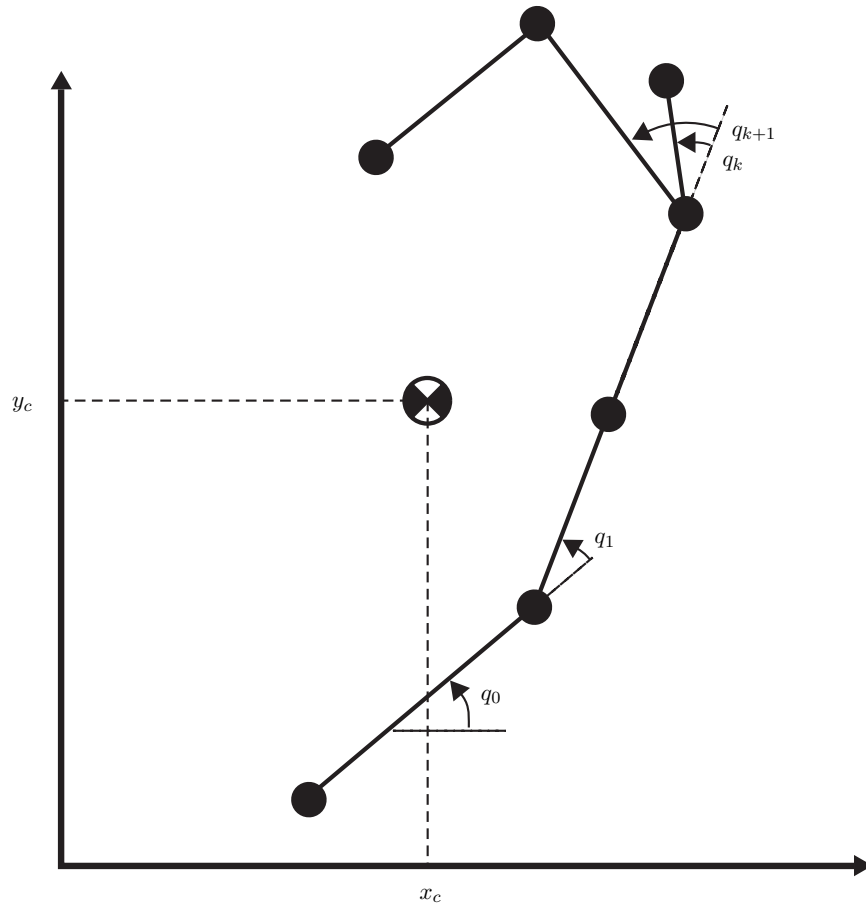


Fig. 2. A planar tree structure in ballistic motion. All joints are actuated. A coordinate convention is indicated. Though not shown, prismatic joints can be included as can springs that act between links but not between a link and the inertial frame.

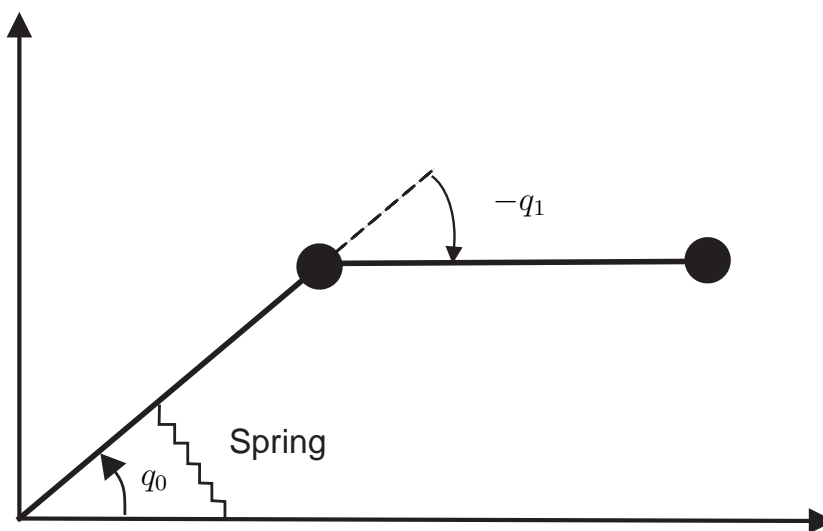


Fig. 3. A two-link robot attached to a pivot and constrained to move in a horizontal plane. The joint q_1 is actuated, while q_0 is passive; a linear spring with stiffness K_s is attached with rest position $q_0 = 0$. From left to right, the links have length L_1 and L_2 and the masses are m_1, m_2 .

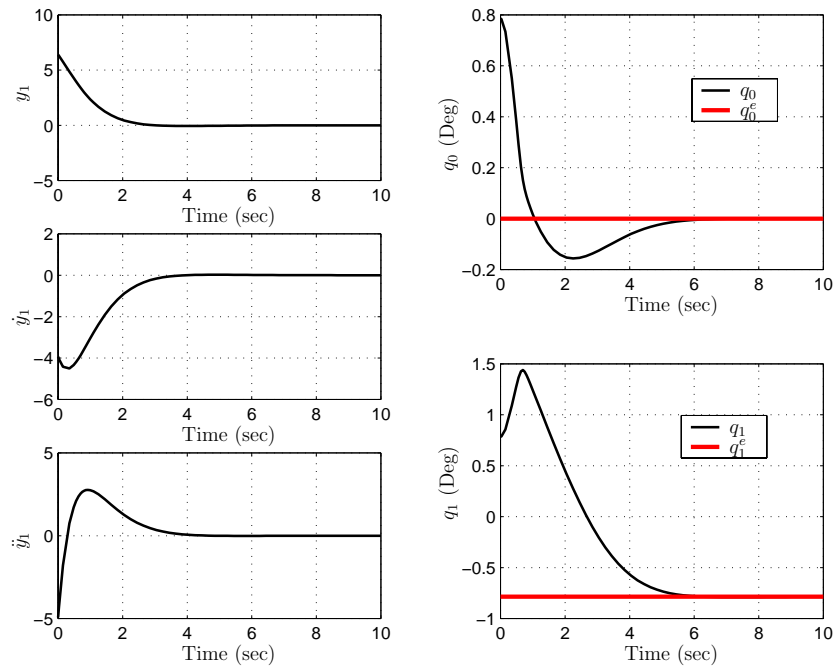


Fig. 4. Stabilization to an equilibrium. The figure shows the convergence of the commanded output, its first two derivatives, and the configuration variables.

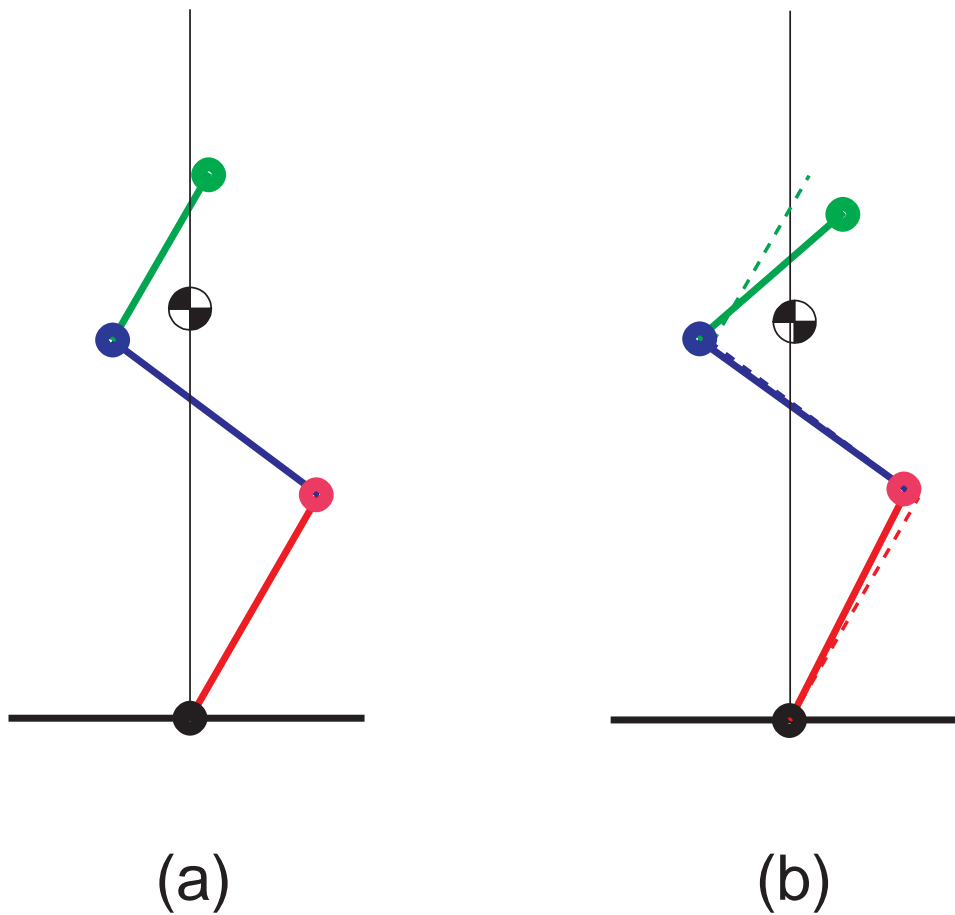


Fig. 5. Three-link mechanism, connected at a pivot, consisting of point masses and massless bars. The links have length L_1 through L_3 starting at the pivot; the masses are m_1 through m_3 . (a) shows an equilibrium pose with the center of gravity centered over the pivot; (b) shows the initial condition used in the simulation, with the equilibrium position superimposed in the background.

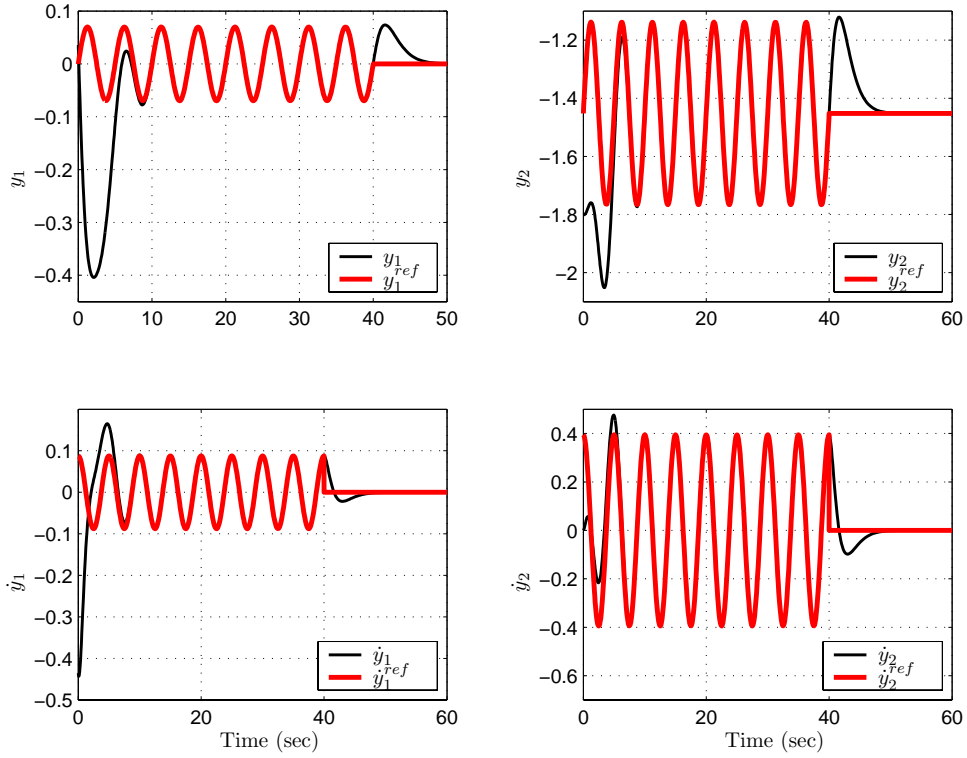


Fig. 6. Demonstration of asymptotic tracking and stabilization for the three-link mechanism. For the first forty seconds, the motion consists of an initial transient, followed by tracking of sinusoidal trajectories that correspond to knee bends. At forty seconds, the reference trajectory is abruptly set to zero, thereby commanding the system to an equilibrium point.

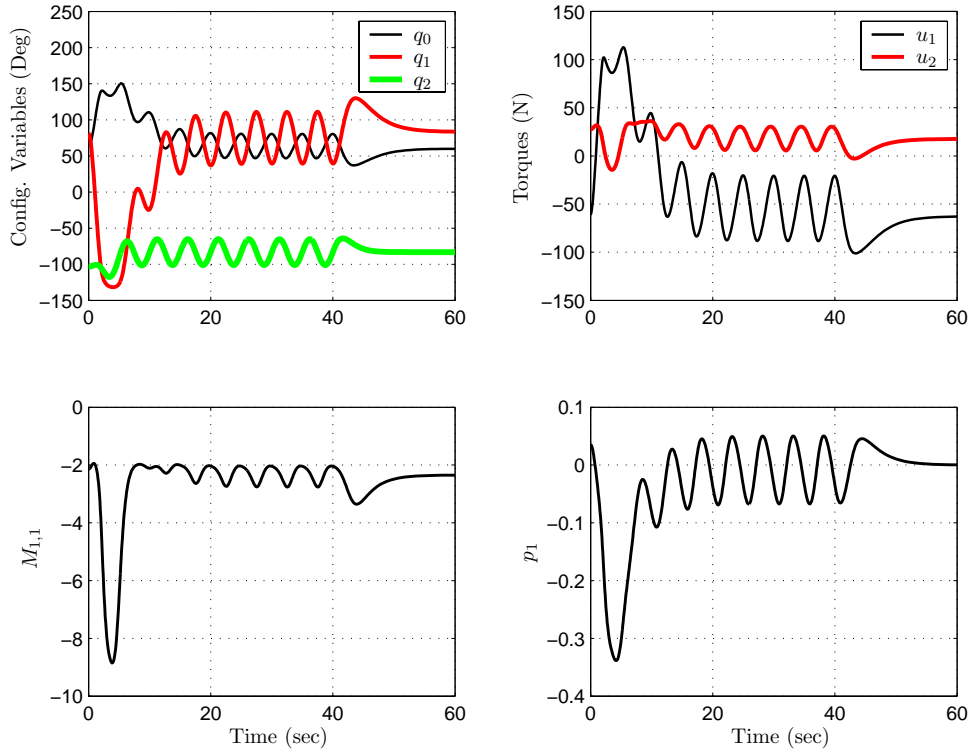


Fig. 7. Demonstration of asymptotic tracking and stabilization for the three-link mechanism; see Figure 6 for details. The plots show the configuration variables (upper left), joint torques (upper right), coefficient that determines invertibility of the decoupling matrix (lower left), and the function that is the key to designing the proper set of outputs (lower right).

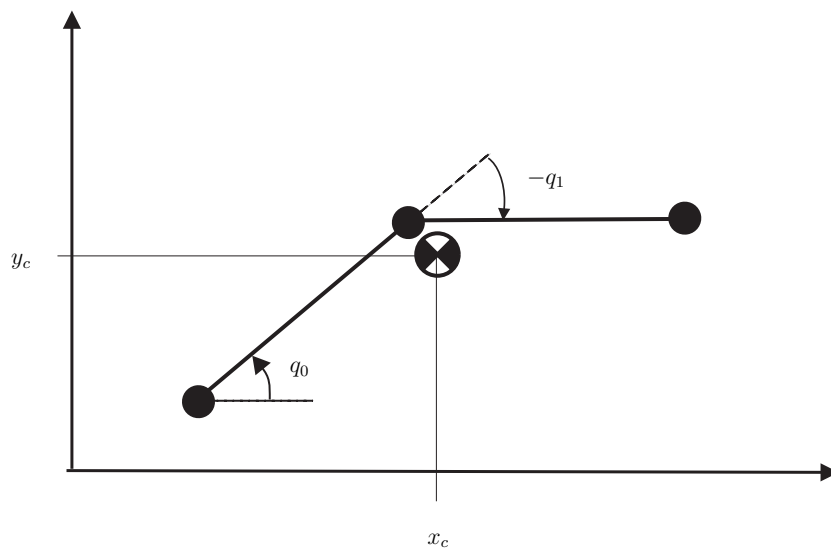


Fig. 8. A two-link robot undergoing ballistic motion in a vertical plane. Only the joint q_1 is actuated. From left to right, the links have length L_1 and L_2 and the masses are m_0, m_1, m_2 .

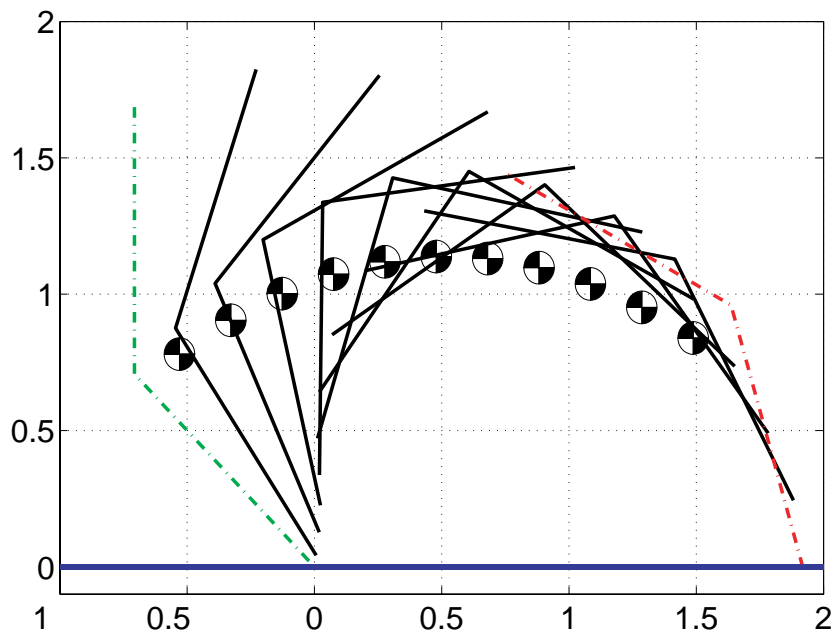


Fig. 9. The motion of the robot passes from left to right without passing through a singularity. The initial configuration ($\cdot - \cdot -$ green) and final configuration ($\cdot - \cdot -$ red) belong to the same configuration class. The center of gravity follows a parabolic trajectory.

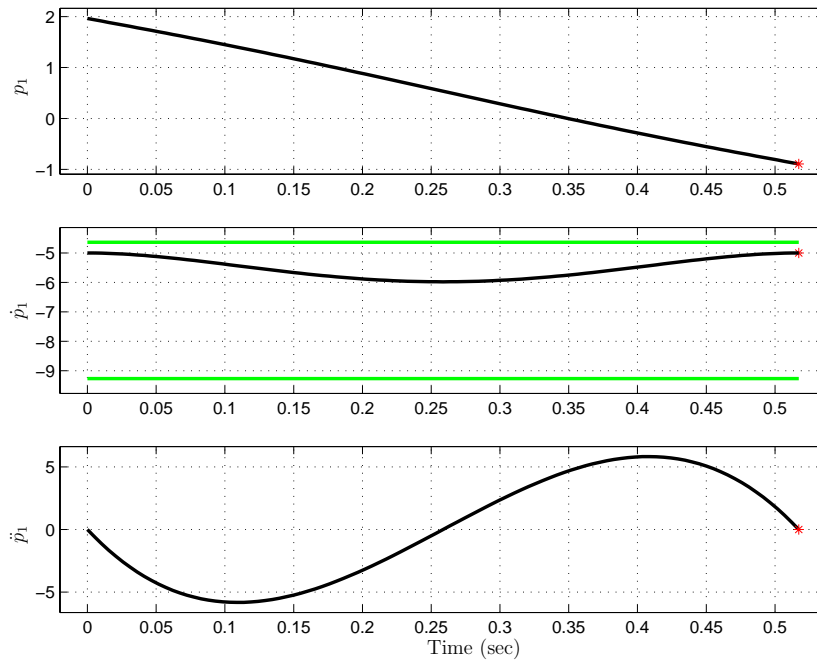


Fig. 10. Based on the initial and final conditions of the flight phase, a trajectory for p_1 and its derivatives is derived. The plot shows that \dot{p} satisfies the constraint $\frac{\sigma}{a_{00}-a_{01}} \leq \dot{p}_1(t) \leq \frac{\sigma}{a_{00}+a_{01}}$

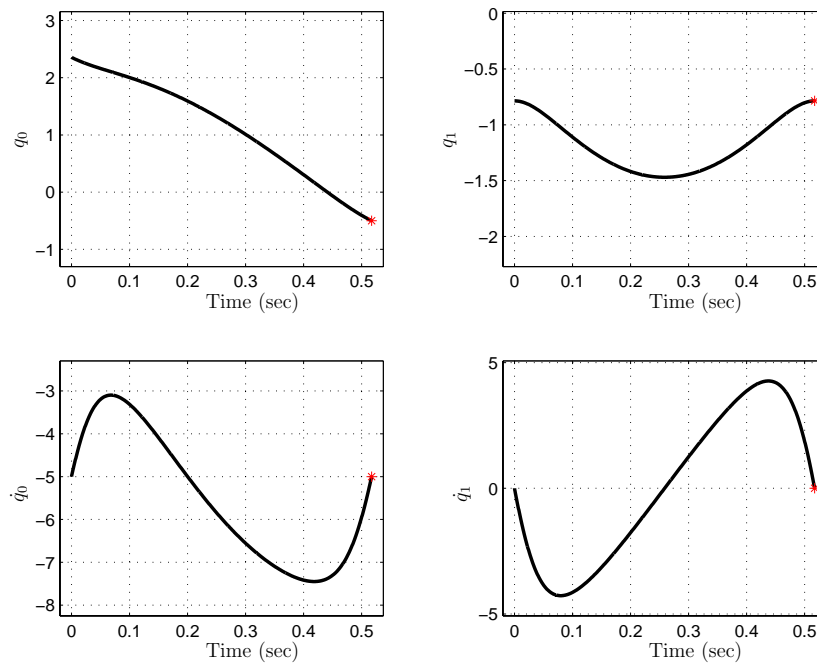


Fig. 11. The computed open-loop control transfers the robot from its initial state to the desired final state (*).

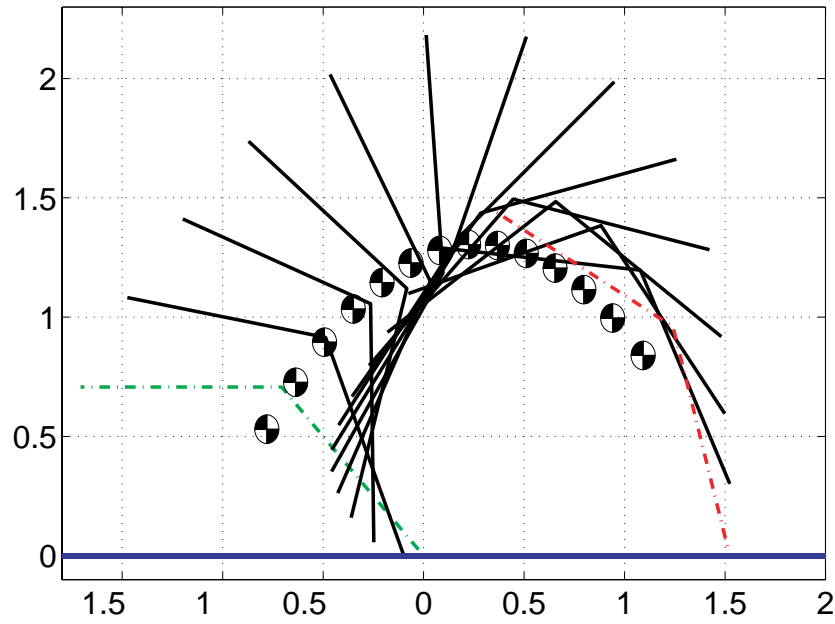


Fig. 12. The motion of the robot passes from left to right, with a singular position occurring when the two links are aligned. The initial configuration (· - · - green) and final configuration (· - · - red) belong to different configuration classes.

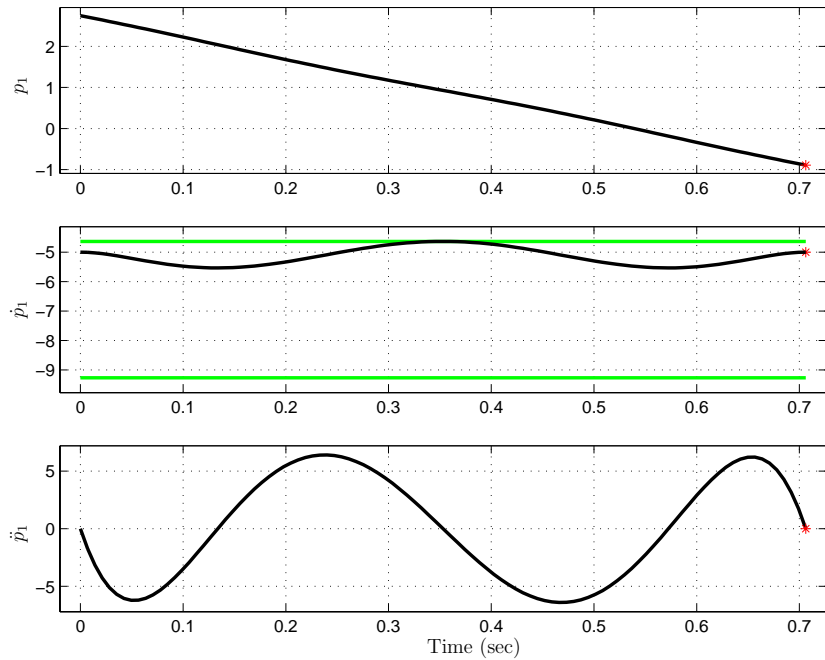


Fig. 13. Based on the initial and final conditions of the flight phase, a trajectory for p_1 and its derivatives is derived. The plot shows that \dot{p}_1 hits the constraint $\frac{\sigma}{a_{00}+a_{01}}$ in the middle of the flight phase, which allows the change in the configuration class to occur.

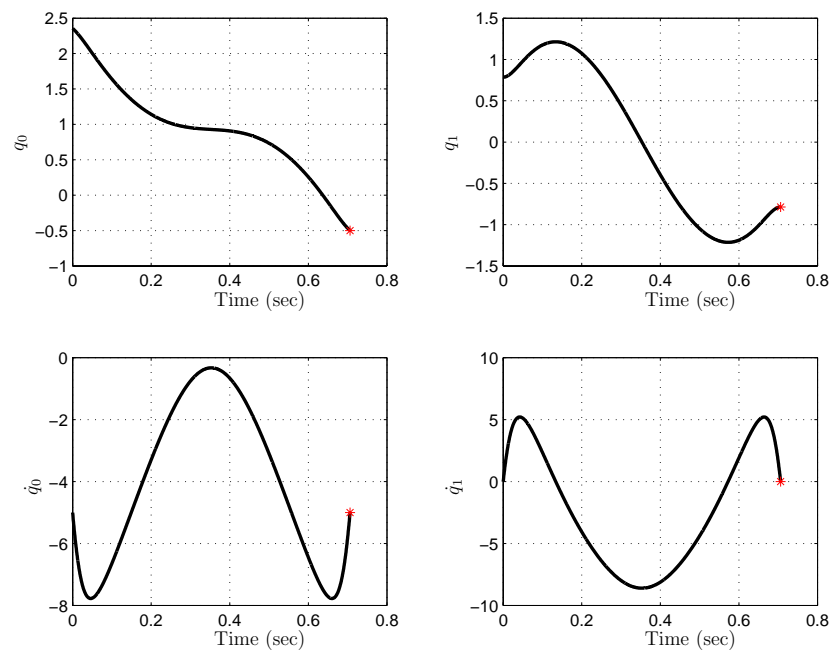


Fig. 14. The computed open-loop control transfers the robot from its initial state to the desired final state (*).